Perturbation Estimation Based Coordinated Adaptive Passive Control for Multimachine Power Systems

B. Yang[a], L. Jiang[a], Wei Yao[b,a], Q. H. Wu[c,a,*]

[a] *Department of Electrical Engineering and Electronics, University of Liverpool, Liverpool, L69 3GJ, United Kingdom*
[b] *State Key Laboratory of Advanced Electromagnetic Engineering and Technology, Huazhong University of Science and Technology, Wuhan, 430074, China*
[c] *School of Electric Power Engineering, South China University of Technology, Guangzhou, 510641, China*

Abstract

This paper proposes a perturbation estimation based coordinated adaptive passive control (PECAPC) of generators excitation system and thyristor-controlled series compensator (TCSC) devices for complex, uncertain and interconnected multimachine power systems. Discussion begins with the PECAPC design, in which the combinatorial effect of system uncertainties, unmodelled dynamics and external disturbances is aggregated into a perturbation term, and estimated online by a perturbation observer (PO). PECAPC aims to achieve a coordinated adaptive control between the excitation controller (EC) and TCSC controller based on the nonlinearly func-

*Corresponding author
Email address: wuqh@scut.edu.cn (Q. H. Wu)

tional estimate of the perturbation. In this control scheme an explicit control Lyapunov function (CLF) and the strict assumption of linearly parametric uncertainties made on power system structures can be avoided. A decentralized stabilizing EC for each generator is firstly designed. Then a TCSC controller is developed to passivize the whole system, which improves system damping through reshaping the distributed energies in power systems. Case studies are carried out on a single machine infinite bus (SMIB) and a three-machine power system, respectively. Simulation results show that the PECAPC-based EC and TCSC controller can coordinate each other to improve the power system stability, finally a hardware-in-the-loop (HIL) test is carried out to verify its implementation feasibility.
Keywords: Coordinated adaptive passive control, perturbation estimation, energy shaping, multimachine power systems.

1. Introduction

Power system stability is becoming a crucial issue as the size and complexity of power systems increase [1]. Conventional linear control methods have been widely used, however, they cannot maintain consistent control performance as power systems are highly nonlinear, which operate under a wide range of operating conditions and various disturbances [2]. Synchronous

generator excitation control is one of the most popular methods to enhance the power system stability. Many nonlinear control approaches have been used for the excitation controller (EC), such as adaptive H_∞ control [3], L-2 disturbance attenuation control [4], nonlinear adaptive control [5], adaptive dynamic programming [6], and optimal predictive control [7]. On the other hand, proper controllers of flexible AC transmission systems (FACTS) can also improve the power system stability. Many studies have been undertaken on the development of nonlinear controllers for thyristor controlled series compensation (TCSC) [8], static variable compensator (SVC) [9], and static synchronous compensator (STATCOM) [10]. However, uncoordinated EC and FACTS controller may deteriorate each other or even lead to instability under large disturbances [1].

To resolve the above issues, many nonlinear coordinated control approaches of excitation systems and FACTS devices have been applied to achieve an optimal performance of the whole system, such as optimal-variable-aim strategies [11], global control [12], and zero dynamics method [13]. However, these methods require accurate system models in the controller design process, which are difficult to guarantee their reliable performances when implemented in a real multimachine system. Hence several adaptive and robust

coordinated control methods are investigated in [14, 15, 16]. However, their design is complicated and cancels possible beneficial nonlinearities. Besides, the optimal control performance may not be obtained as the physical property of a power system is ignored.

Passivity provides a physical insight for the analysis and design of nonlinear systems, which decomposes a complex nonlinear system into simpler subsystems that, upon interconnection, and adds up their local energies to determine the full system's behavior. The action of a controller connected to the dynamical system may also be regarded, in terms of energy, as another separate dynamical system. Thus the control problem can then be treated as finding an interconnection pattern between the controller and the dynamical system. This 'energy shaping' approach is the essence of passive control (PC), which takes into account the energy of the system and gives a clear physical meaning, such that the changes of the overall storage function can take a desired form [17, 21]. It is well known that the nature of a power system is to produce, transmit and consume energy, and the power flow into the network must be greater than or equal to the rate of change of the energy stored in the network [18]. Coordinated passive control (CPC) [19, 20] is an extended passivity-based method [22, 23], which requires an accurate system model.

Therefore, coordinated adaptive passive control (CAPC) has been developed for the control of generators and TCSCs by [24, 25]. However, it is based on the linearly parametric adaption, which updating law can only deal with an uncertain damping coefficient and a nonlinear TCSC unmodelled dynamics satisfying a linear growth condition. These assumptions restrict its application in real multimachine system operations as the modelling uncertainty consists of the inertial constant, time constant, general unmodelled TCSC dynamics and inter-area oscillation. Moreover, an explicit control Lyapunov function (CLF) needs to be constructed which is difficult in multimachine systems.

Perturbation observer (PO) has been proposed to estimate the lumped uncertainty not considered in the nominal plant model, based on an extended state space model [26, 27, 5, 29, 30], such as sliding-mode control with perturbation estimation (SMCPE) which uses a sliding-mode perturbation observer (SMPO) to reduce the conservativeness of the sliding-mode control (SMC) [26], active disturbance rejection controller (ADRC) which designs nonlinear disturbance observers [27], and a high-gain perturbation observer (HGPO) or SMPO as an extended-order linear observer [5, 29, 30]. This paper adopts the HGPO as it provides convenience of stability analysis of closed-loop sys-

tem, as the SMPO [26] may suffer the discontinuity of high-speed switching and the nonlinear observer [27] is too complex for stability analysis.

Main contributions of this paper are highlighted as follows:

• A perturbation estimation based coordinated adaptive passive control (PECAPC) scheme has been proposed, via designing a PO to achieve a functional estimation and compensation. It can partially releases the dependence of system model in the passive control (PC) and handle time-varying unknown dynamic, while conventional adaptive passive control (APC) [24, 25] can only estimate the linearly parametric uncertainties.

• The design of PECAPC is relatively simpler than that of the APC as it only requires the range of control Lyapunov function (CLF), while APC requires an explicit CLF which is difficult to find in complex nonlinear systems.

• The proposed PECAPC scheme is applied for both single machine infinite bus (SMIB) and multimachine power systems, without requiring the accurate model of a large-scale power system, in which APC cannot be applied due to the unavailability of accurate model.

• The effectiveness of the proposed controller is verified by simulation and hardware-in-the-loop (HIL) tests.

Analysis begins with decomposing the original power system into several subsystems, in which the TCSC reactance and its modulated input are chosen as the system output and input, respectively, such that the relative degree is one. A decentralized stabilizing EC for each generator is designed at first, the uncertain parameters and unmodelled dynamics of generator are lumped into a perturbation which is estimated and compensated by a high-gain state and perturbation observer (HGSPO). Then a coordinated TCSC controller is developed via passivation to ensure the whole system stability, the uncertain TCSC parameters and general unmodelled TCSC dynamics are aggregated into another perturbation, which is estimated and compensated by a HGPO. Two case studies are undertaken on a single machine infinite bus (SMIB) and a three-machine system to evaluate the effectiveness of PECAPC, respectively. Simulation and HIL test results are provided to verify the effectiveness of the proposed approach.

2. Power Plant Model

2.1. A Single Machine Infinite Bus System with a TCSC Device

A SMIB system with a TCSC device is shown in Fig. A.1, of which the system dynamics is described as [24]

$$\begin{cases} \dot{\delta} = \omega - \omega_0 \\ \dot{\omega} = -\frac{D}{H}(\omega - \omega_0) + \frac{\omega_0}{H}\left(P_{\mathrm{m}} - \frac{E'_{\mathrm{q}} V_{\mathrm{s}} \sin\delta}{X'_{\mathrm{d}\Sigma} + X_{\mathrm{tcsc}}}\right) \\ \dot{E}'_{\mathrm{q}} = \frac{(X_{\mathrm{d}} - X'_{\mathrm{d}})(V_{\mathrm{s}}\cos\delta - E'_{\mathrm{q}})}{T_{\mathrm{d0}}(X'_{\mathrm{d}\Sigma} + X_{\mathrm{tcsc}})} - \frac{1}{T_{\mathrm{d0}}} E'_{\mathrm{q}} + \frac{K_{\mathrm{c}}}{T_{\mathrm{d0}}} u_{\mathrm{fd}} \\ \dot{X}_{\mathrm{tcsc}} = -\frac{1}{T_{\mathrm{c}}}(X_{\mathrm{tcsc}} - X_{\mathrm{tcsc0}}) + \frac{K_{\mathrm{T}}}{T_{\mathrm{c}}} u_{\mathrm{c}} + \zeta_{\mathrm{tcsc}} \end{cases} \tag{1}$$

where δ and ω denote the angle and relative speed of the generator rotor, respectively; H the inertia constant; P_{m} the constant mechanical power on the generator shaft; D the damping coefficient; E'_{q} and V_{s} the inner generator voltage and infinite bus voltage; T_{d0} the d-axis transient short-circuit time constant; T_{c} the time constant of TCSC; $X'_{\mathrm{d}\Sigma} = X_{\mathrm{t}} + X'_{\mathrm{d}} + \frac{1}{2}(X_{\mathrm{L1}} + X_{\mathrm{L2}})$; X_{t} the transformer reactance; X'_{d} the d-axis generator transient reactance; X_{L1} and X_{L2} the transmission line reactance; X_{tcsc} the TCSC reactance and X_{tcsc0} the initial TCSC reactance; K_{c} the gain of excitation amplifier; u_{fd} the excitation voltage; K_{T} the gain of TCSC regulator; u_{c} the TCSC modulated input; and ζ_{tcsc} the unmodelled TCSC dynamics.

2.2. A Multimachine System with a TCSC Device

A multimachine system with n machines and a TCSC device, where the nth machine is the reference machine, is described by [5]

$$\begin{cases} \dot{\delta}_i = \omega_i - \omega_0 \\ \dot{\omega}_i = \frac{\omega_0}{2H_i}\left(P_{\mathrm{m}i} - \frac{D_i}{\omega_0}(\omega_i - \omega_0) - P_{\mathrm{e}i}\right) \\ \dot{E}'_{\mathrm{q}i} = \frac{1}{T_{\mathrm{d0}i}}(u_{\mathrm{fd}i} - E_{\mathrm{q}i}), \qquad i = 1, 2, \cdots, n, \\ \dot{X}_{\mathrm{tcsc}} = -\frac{1}{T_{\mathrm{c}}}(X_{\mathrm{tcsc}} - X_{\mathrm{tcsc0}}) + \frac{K_{\mathrm{T}}}{T_{\mathrm{c}}}u_{\mathrm{c}} + \zeta_{\mathrm{tcsc}} \end{cases} \tag{2}$$

with

$$\begin{aligned} E_{\mathrm{q}i} &= E'_{\mathrm{q}i} + (x_{\mathrm{d}i} - x'_{\mathrm{d}i})I_{\mathrm{d}i} \\ P_{\mathrm{e}i} &= E'_{\mathrm{q}i}I_{\mathrm{q}i} + E'^2_{\mathrm{q}i}G_{ii} \\ I_{\mathrm{d}i} &= -\sum_{j=1, j\neq i}^{n} E'_{\mathrm{q}j}Y_{ij}\cos(\delta_i - \delta_j) \\ I_{\mathrm{q}i} &= -\sum_{j=1, j\neq i}^{n} E'_{\mathrm{q}j}Y_{ij}\sin(\delta_i - \delta_j) \end{aligned}$$

where subscript i denotes the variables of the ith machine; δ_i the relative rotor angle; ω_i the generator rotor speed; $E_{\mathrm{q}i}$ and $E'_{\mathrm{q}i}$ the voltage and transient voltage on the q-axis; $P_{\mathrm{m}i}$ the constant mechanical power input; $P_{\mathrm{e}i}$ the electrical power output; H_i the rotor inertia; $T_{\mathrm{d0}i}$ the d-axis transient short-

circuit time constant; $I_{\mathrm{d}i}$ and $I_{\mathrm{q}i}$ the d-axis and q-axis generator current; Y_{ij} the equivalent admittance between the ith and jth nodes, which is modified as $Y'_{ij} = 1/(1/Y_{ij} + X_{\mathrm{tcsc}})$ when a TCSC is equipped between the ith and jth nodes; and G_{ii} the equivalent self conductance of the ith machine.

3. Perturbation Estimation based Coordinated Adaptive Passive Control

Consider a two input system in formal form of passive system as follows [19, 21]:

$$\dot{z} = Az + B(a(z, y) + b(z, y)u_2 + \xi) \tag{3}$$

$$\dot{y} = \alpha(z, y) + \beta_1(z, y)u_1 + \beta_2(z, y)u_2 + \zeta \tag{4}$$

where $y \in \mathbb{R}$ is the output and the relative degree from u_1 to y is one, which is the basic form in CPC design. $z \in \mathbb{R}^{n-1}$ is the state vector of the internal dynamics; $a(z, y) : \mathbb{R}^{n-1} \times \mathbb{R} \to \mathbb{R}$ and $b(z, y) : \mathbb{R}^{n-1} \times \mathbb{R} \to \mathbb{R}$ are C^∞ unknown smooth functions, $\xi \in \mathbb{R}$ and $\zeta \in \mathbb{R}$ are modelling uncertainties. $\alpha(z, y)$, $\beta_1(z, y)$ and $\beta_2(z, y)$ are all unknown functions defined on $\mathbb{R}^{n-1} \times \mathbb{R}$.

Matrices A and B are

$$A = \begin{bmatrix} 0 & 1 & 0 & \cdots & 0 \\ 0 & 0 & 1 & \cdots & 0 \\ \vdots & & & & \vdots \\ 0 & 0 & 0 & \cdots & 1 \\ 0 & 0 & 0 & \cdots & 0 \end{bmatrix}_{(n-1)\times(n-1)}, \quad B = \begin{bmatrix} 0 \\ 0 \\ \vdots \\ 0 \\ 1 \end{bmatrix}_{(n-1)\times 1}$$

The zero dynamics of system (3) is assumed to be stabilizable by u_2 and written as

$$\dot{z} = Az + B(a(z,0) + b(z,0)u_2 + \xi) \tag{5}$$

3.1. Design of HGSPO and HGPO [5]

The perturbation of system (5) is defined as

$$\Psi_1(\cdot) = a(z,0) + (b(z,0) - b_{10})u_2 + \xi \tag{6}$$

Define a fictitious state to represent the system perturbation, that is, $z_n = \Psi_1(\cdot)$. Then extend the original $(n-1)$th-order system (5) into the following

nth-order system

$$\dot{z}_{\mathrm{e}} = A_1 z_{\mathrm{e}} + B_1 u_2 + B_2 \dot{\Psi}_1(\cdot) \tag{7}$$

where $z_{\mathrm{e}} = [z_1, z_2, \cdots, z_{n-1}, z_n]^{\mathrm{T}}$. $B_1 = [0, 0, \ldots, b_{10}, 0]^{\mathrm{T}} \in \mathbb{R}^n$ and $B_2 = [0, 0, \ldots, 1]^{\mathrm{T}} \in \mathbb{R}^n$. Matrix A_1 is

$$A_1 = \begin{bmatrix} 0 & 1 & \cdots & \cdots & 0 \\ 0 & 0 & 1 & \cdots & 0 \\ \vdots & & & & \vdots \\ 0 & 0 & 0 & \cdots & 1 \\ 0 & 0 & 0 & \cdots & 0 \end{bmatrix}_{n \times n}$$

Throughout this paper, $\tilde{x} = x - \hat{x}$ refers to the estimation error of x whereas $\hat{x}$ represents the estimate of x. A nth-order HGSPO is used for the extended nth-order system (7) as

$$\dot{\hat{z}}_{\mathrm{e}} = A_1 \hat{z}_{\mathrm{e}} + B_1 u_2 + H(z_1 - \hat{z}_1) \tag{8}$$

where $H = [\alpha_1/\epsilon, \alpha_2/\epsilon^2, \cdots, \alpha_{n-1}/\epsilon^{n-1}, \alpha_n/\epsilon^n]^{\mathrm{T}}$ is the observer gain with $0 < \epsilon < 1$.

The estimation errors of HGSPO (8) is calculated as

$$\dot{\tilde{z}}_{\mathrm{e}} = A_1 \tilde{z}_{\mathrm{e}} + B_2 \dot{\Psi}_1(\cdot) - H(z_1 - \hat{z}_1)$$

The design procedure of HGSPO can be summarized as following steps:

Step 1: Define the perturbation for system (5) as Eq. (6);

Step 2: Define a fictitious state to represent the perturbation as $z_n = \Psi_1(\cdot)$;

Step 3: Extend the original (n-1)th-order system (5) into the extended nth-order system (7);

Step 4: Design a nth-order HGSPO (8) to estimate state z and perturbation $\Psi_1(\cdot)$ for the extended nth-order system (7);

Step 5: Choose $\alpha_i = C_n^i \lambda^i$ such that the pole of HGSPO (8) can be placed at $-\lambda$, where $i = 1, 2, \cdots, n$ and $\lambda > 0$.

Similarly, the perturbation of system (4) is defined as

$$\Psi_2(\cdot) = \alpha(z, y) + \beta_2(z, y) u_2 + (\beta_1(z, y) - b_{20}) u_1 + \zeta \tag{9}$$

Define a fictitious state to represent the system perturbation, that is, $y_2 =$

$\Psi_2(\cdot)$. Then extend the original first-order system (4) into the following second-order system

$$\begin{cases} \dot{y} = y_2 + b_{20}u_1 \\ \dot{y}_2 = \dot{\Psi}_2(\cdot) \end{cases} \tag{10}$$

A second-order HGPO is used for system (10) as

$$\begin{cases} \dot{\hat{y}} = \hat{\Psi}_2 + \frac{\alpha'_1}{\epsilon'}(y - \hat{y}) + b_{20}u_1 \\ \dot{\hat{\Psi}}_2(\cdot) = \frac{\alpha'_2}{\epsilon'^2}(y - \hat{y}) \end{cases} \tag{11}$$

where $0 < \epsilon' < 1$.

Define the scaled estimation errors of HGPO (11) as $\eta'_1 = \tilde{y}/\epsilon'$, $\eta'_2 = \tilde{\Psi}_2(\cdot)$, and $\eta' = [\eta'_1, \eta'_2]^{\mathrm{T}}$, gives

$$\epsilon'\dot{\eta}' = A'_1\eta' + \epsilon' B'_1\dot{\Psi}_2(\cdot) \tag{12}$$

with

$$A'_1 = \begin{bmatrix} -\alpha'_1 & 1 \\ -\alpha'_2 & 0 \end{bmatrix}, \quad B'_1 = \begin{bmatrix} 0 \\ 1 \end{bmatrix}$$

where α'_1 and α'_2 are chosen such that A'_1 is a Hurwitz matrix.

The design procedure of HGPO is similar to that of HGSPO. Normally

the pole of HGSPO (8) and HGPO (11) is chosen to be 10 times larger than the dominant pole of the equivalent linear system of (5) and (4), respectively, which can ensure a fast estimation of perturbation $\Psi_1(\cdot)$ and $\Psi_2(\cdot)$. Note that one only needs the measurement of state z_1 and input u_2 for the design of HGSPO (8), and the measurement of output y and input u_1 for the design of HGPO (11). The effectiveness of the PO has been discussed in our previous work [5, 29, 30].

Remark 1. It should be mentioned that during the design procedure, ϵ and ϵ' used in HGSPO (8) and HGPO (11) are required to be some relatively small positive constants only, and the performance of HGSPO and HGPO is not very sensitive to the observer gains, which are determined based on the upper bound of the derivative of perturbation.

3.2. Design of stabilizing controller u_2 and coordinated controller u_1

Based on the standard CPC design procedure [19], the stabilizing controller u_2 is designed first as follows:

$$u_2 = \gamma(\hat{z}_{\mathrm{e}}) = \frac{1}{b_{10}}(-K\hat{z} - \hat{z}_n) \tag{13}$$

which renders system (3) into

$$\dot{z} = Az + B(a(z,y) + b(z,y)\gamma(\hat{z}_{\mathrm{e}}) + \xi) = \tilde{q}(z) + \tilde{p}(z,y)y$$

with

$$\tilde{q}(z) = Az + B(a(z,0) + b(z,0)\gamma(\hat{z}_{\mathrm{e}}) + \xi) \tag{14}$$

and

$$\tilde{p}(z,y) = B(a(z,y) - a(z,0) + (b(z,y) - b(z,0))\gamma(\hat{z}_{\mathrm{e}}))y^{-1} \tag{15}$$

where $\tilde{q}(z)$ represents the zero dynamics, $\tilde{p}(z,y)$ denotes the difference between the original system and zero dynamics, which will be cancelled later by u_1. $K = [k_1, k_2, \cdots, k_{n-1}]$ is the control gain which makes matrix $A - BK$ Hurwitzian, such that the following condition can be satisfied

$$\dot{W} = \frac{\partial W(z)}{\partial z^{\mathrm{T}}}\tilde{q}(z) + \frac{\partial W}{\partial \eta^{\mathrm{T}}}\dot{\eta} \leq -\alpha(\|z\|) \tag{16}$$

where α is a class-$\mathcal{K}$ function, and $\eta = [\tilde{z}_1/\epsilon^{n-1}, \tilde{z}_2/\epsilon^{n-2}, \cdots, \tilde{z}_n] \in \mathbb{R}^n$.

The proof of inequality (16) is given in [5].

The structure of stabilizing controller (13) is illustrated in Fig. A.2. The nominal plant is disturbed by the perturbation $\Psi_1(\cdot)$, the stabilizing controller u_2 can be separated as $u_2 = b_{10}^{-1}(u_{s1} + u_{s2})$, where $u_{s1} = -K\hat{z}$ is the state feedback and choose $k_i = C_{n-1}^i \xi^i$ to place the pole of the equivalent linear system of (5) at $-\xi$, where $i = 1, ..., n-1$ and $\xi > 0$; and $u_{s2} = -\hat{z}_n$ compensates the combinatorial effect of parameter uncertainties, external disturbances and unmodelled dynamics.

The coordinated controller u_1 is designed as

$$\begin{cases} u_1 = b_{20}^{-1}\left(-\hat{\Psi}_2(\cdot) - k'y - \frac{\partial W}{\partial z^{\mathrm{T}}}\tilde{p}(z,y) + \nu\right) \\ \nu = -\phi(y) \end{cases} \tag{17}$$

where ν is the additional input, ϕ is any smooth function such that $\phi(0) = 0$ and $y\phi(y) > 0$ for all $y \neq 0$. $k' > 1$ is the feedback control gain.

The structure of coordinated controller (17) is illustrated in Fig. A.3. The nominal plant is disturbed by the perturbation $\Psi_2(\cdot)$, the coordinated controller u_1 can be separated as $u_1 = b_{20}^{-1}(u_{c1} + u_{c2} + u_{c3} + u_{c4})$, where $u_{c1} = -\hat{\Psi}_2(\cdot)$ is the dynamical perturbation compensation; $u_{c2} = -k'y$ places the pole of the equivalent linear system of (4) at $-k'$, where $k' > 0$;

$u_{c3} = \frac{\partial W}{\partial z^{\mathrm{T}}}\tilde{p}(y,z)$ coordinates the two controllers by cancelling the difference between the original system and zero dynamics represented by $\tilde{p}(y,z)$; and $u_{c4} = \nu$ constructs a passive system by introducing an additional input in the form of a sector-nonlinearity $\phi(y)$.

Remark 2. Note that $\frac{\partial W(z)}{\partial z^{\mathrm{T}}}\tilde{p}(z,y) = \frac{\partial W(z)}{\partial z_{n-1}}\tilde{p}_{n-1}(z,y)$ as $\tilde{p}_i(z,y) = 0$, $i = 1, 2, \cdots, n-2$, which can be interpreted as the distributed energies in a complex system and needs to be reshaped. One can choose $\frac{\partial W(z)}{\partial z^{\mathrm{T}}}\tilde{p}(z,y) = cz_{n-1}\tilde{p}_{n-1}(z,y)$ regardless of the system order, where c is called the coordination coefficient.

Remark 3. For the closed-loop system (18), control gain k' should be designed to suppress the perturbation estimation error $\tilde{\Psi}_2(\cdot)$. Compared to the approach without perturbation compensation, in which k' should be chosen to suppress the perturbation $\Psi_2(\cdot)$. As $\Psi_2(\cdot)$ is normally larger than $\tilde{\Psi}_2(\cdot)$, a smaller k' could be resulted in due to the compensation of perturbation by PECAPC.

To this end, PECAPC design for systems (3) and (4) can be summarized as:

Step 1: Obtain zero dynamics (5) of system (3) by setting $y = 0$

Step 2: Extend system (5) into system (7), and design HGSPO (8) to obtain estimates $\hat{z}$ and $\hat{z}_n$

Step 3: Design stabilizing controller (13)

Step 4: Extend system (4) into system (10), and design HGPO (11) to obtain the estimate $\hat{\Psi}_2(\cdot)$

Step 5: Design coordinated controller (17)

3.3. Closed-loop system stability

The proof of stability of the closed-loop system with control stabilizing controller u_2 and coordinated controller u_1 is given in the following Theorem 1.

Theorem 1. *Consider systems (3) and (4), with controllers (13) and (17), and let assumptions A1 and A2 hold; then* $\exists\epsilon_1^*$, $\epsilon_1^* > 0$ *such that,* $\forall\epsilon'$, $0 < \epsilon' < \epsilon_1^*$, *then the closed-loop system is passive and its origin is stable.*

The following assumptions are made on systems (7) and (10).

A1. b_{10} and b_{20} are chosen to satisfy:

$$0 < |b(z,0)/b_{10} - 1| \leq \theta_1, \quad 0 < |\beta_1(z,y)/b_{20} - 1| \leq \theta_2$$

where $\theta_1 < 1$ and $\theta_2 < 1$ are positive constants.

A2. The perturbation $\Psi_k(\cdot)$ and its derivative $\dot{\Psi}_k(\cdot)$ are Lipschitz in their arguments and bounded over the domain of interest and are globally bounded in (z, y):

$$|\Psi_k(z, y, u)| \leq \gamma_1, \quad |\dot{\Psi}_k(z, y, u)| \leq \gamma_2$$

where γ_1 and γ_2 are positive constants. In addition, $\Psi_k(0, 0, 0) = 0$, $\dot{\Psi}_k(0, 0, 0) = 0$, $k = 1, 2$. It guarantees that the origin is an equilibrium point of the open-loop system.

Proof. The closed-loop system (4) using controller (17) is

$$\begin{cases} \dot{y} = \eta_2' - k'y - \frac{\partial W(z)}{\partial z^{\mathrm{T}}}\tilde{p}(z, y) + \nu \\ \epsilon'\dot{\eta}' = A_1'\eta' + \epsilon' B_1'\dot{\Psi}_2(\cdot) \end{cases} \tag{18}$$

Define a Lyapunov function $V(\eta') = \eta'^{\mathrm{T}} P_1 \eta'$, where P_1 is the positive definite solution of the Lyapunov equation $P_1 A_1' + A_1'^{\mathrm{T}} P_1 = -I$. For closed-loop systems (3) and (4) by controllers (13) and (17), we choose a storage function

as

$$H(z,\eta,y,\eta') = W(z,\eta) + \frac{1}{2}y^2 + \beta V(\eta') \tag{19}$$

where $\beta > 0$. Moreover, assuming

$$\|\dot{\Psi}_2(\cdot)\| \leq L_1\|y\| + L_2\|\eta'\|$$

where L_1 and L_2 are Lipschitz constants.

By differentiating $H(z,\eta,y,\eta')$ along the trajectory of system (18) and condition (16), it yields

$$\begin{aligned}
\dot{H} &= \frac{\partial W}{\partial z^{\mathrm{T}}}(\tilde{q}(z) + \tilde{p}(z,y)y) + \frac{\partial W}{\partial \eta^{\mathrm{T}}}\dot{\eta} + y\Big(\eta_2' - k'y - \frac{\partial W}{\partial z^{\mathrm{T}}}\tilde{p}(z,y) + \nu\Big) \\
&\quad + \beta\frac{\partial V}{\partial \eta'^{\mathrm{T}}}\left(\frac{A_1'\eta'}{\epsilon'} + B_1'\dot{\Psi}_2(\cdot)\right) \\
&\leq -\alpha(\|z\|) + y\nu - \|y\|^2 - \frac{\beta}{\epsilon'}\|\eta'\|^2 + 2\beta L_2\|P_1\|\|\eta'\|^2 + (1 + 2\beta L_1\|P_1\|)\|y\|\|\eta'\| \\
&\leq -\alpha(\|z\|) + y\nu - \|y\|^2 - \frac{\beta}{\epsilon'}\|\eta'\|^2 + 2\beta L_2\|P_1\|\|\eta'\|^2 + (1 + 2\beta L_1\|P_1\|) \\
&\quad \times \left(\frac{1}{\epsilon_0}\|y\|^2 + \epsilon_0\|\eta'\|^2\right) \\
&\leq -\alpha(\|z\|) + y\nu - \frac{1}{2}\|y\|^2 - \frac{\beta}{2\epsilon'}\|\eta'\|^2 - b_1\|y\|^2 - b_2\|\eta'\|^2
\end{aligned}$$

where

$$b_1 = \frac{1}{2} - \frac{2}{\epsilon_0}\left(\frac{1}{2} + \beta L_1 \|P_1\|\right), \qquad b_2 = \frac{\beta}{2\epsilon'} - 2\beta(\epsilon_0 L_1 + L_2)\|P_1\| - \epsilon_0$$

with $\epsilon_0 > 0$. One can choose β small enough and $\epsilon_0 \geq \epsilon_0^* = 2 + 4\beta L_1 \|P_1\|$ such that $b_1 > 0$, then choose $\epsilon_1^* = \beta/(\epsilon_0^{*2} + 4\beta L_2 \|P_1\|)$, $\forall \epsilon', \epsilon' \leq \epsilon_1^*$, and choose the additional input $\nu = -\phi(y)$, where $\phi(y)$ is a sector-nonlinearity satisfying $y\phi(y) > 0$. It can be shown that

$$\begin{aligned}\dot{H} &\leq -\alpha(\|z\|) - \min(1/2, \beta/2\epsilon')(\|y\|^2 + \|\eta'\|^2) + y\nu \leq -\alpha(\|z\|) - \alpha_1(\|y\|) + y\nu \\ &\leq y\nu \leq -y\phi(y) \leq 0\end{aligned}$$

where α_1 is a class-$\mathcal{K}$ function. One can conclude that the closed-loop system is passive and its origin is stable. □

Proposition 1. PECAPC can be easily extended into multi-input systems. If there exists m subsystems for system (3) with m control inputs u_{2j}, the vector variables of states and estimation errors for each subsystem are denoted as z_j^* and η_j^*, $j = 1, 2, \cdots, m$, respectively. Controller (13) using HGSPO (8) can decouple each subsystem by rendering their interactions into a per-

turbation. Hence u_{2j} can stabilize the jth subsystem, which results in an equivalent CLF $W(z^*, \eta^*) = W_1 + W_2 + \cdots + W_m$, and condition (16) becomes

$$\dot{W} = \sum_{j=1}^{m} \left(\frac{\partial W}{\partial z_j^{*\mathrm{T}}} \tilde{q}_j(z_j^*) + \frac{\partial W}{\partial \eta_j^{*\mathrm{T}}} \dot{\eta}_j^* \right) \leq \sum_{j=1}^{m} \alpha_j(\|z_j^*\|)$$

Remark 4. Denote $(z_0, y_0) \in \Gamma_{\mathrm{o}}$ and $z_0' \in \Gamma_{\mathrm{z}}$ as the equilibrium point of systems (3) and (5), respectively, where Γ_{o} and Γ_{z} are their stability region, which are unequal during transient process. However, with a proper coordination coefficient c, passive controller (17) will exponentially drive $\lim_{t\to\infty}(z_0, y_0) = z_0'$ and $\lim_{t\to\infty} \Gamma_{\mathrm{o}} = \Gamma_{\mathrm{z}}$ as $\lim_{t\to\infty} y = 0$.

Remark 5. Compared to the CAPC [24, 25] which usually estimates the linearly parametric uncertainties, the PECAPC can be regarded as a nonlinearly functional estimation method, as it can estimate the combinatorial effect of fast time-varying unknown parameters, unknown nonlinear dynamics and external disturbances. If there does not exist uncertainties and external disturbances, and if the accurate system model is available, such a controller provides the same performance as the exact passive controller. Otherwise, such a controller performs much better than the exact passive controller.

The use of PO leads to less concern over the measurement and identification of the fast time-varying unknown parameters, unknown nonlinear dynamics and external disturbances. This tends to require less control efforts as the perturbation has already included all of this information.

4. PECAPC Design of Excitation and TCSC

Controllers (13) and (17) will be applied for both SMIB system (1) and multimachine system (2).

4.1. Controller Design for a Single Machine Infinite Bus System

For SMIB system (1), we chose $y = X_{\rm tcsc} - X_{\rm tcsc0}$, $u_1 = u_{\rm c}$ and $u_2 = u_{\rm fd}$. By setting $y = 0$, the zero dynamics of system (1) is

$$\begin{cases} \dot{\delta} = \omega - \omega_0 \\ \dot{\omega} = -\frac{D}{H}(\omega - \omega_0) + \frac{\omega_0}{H}\left(P_{\rm m} - \frac{E'_{\rm q} V_{\rm s} \sin\delta}{X'_{\rm d\Sigma} + X_{\rm tcsc0}}\right) \\ \dot{E}'_{\rm q} = \frac{(X_{\rm d} - X'_{\rm d})(V_{\rm s}\cos\delta - E'_{\rm q})}{T_{\rm d0}(X'_{\rm d\Sigma} + X_{\rm tcsc0})} - \frac{1}{T_{\rm d0}} E'_{\rm q} + \frac{K_{\rm c}}{T_{\rm d0}} u_{\rm fd} \end{cases} \tag{20}$$

Choose $z_1 = \delta - \delta_0$ for system (20), where δ_0 is the initial generator rotor angle. Differentiating z_1 until the excitation control input $u_{\rm fd}$ appears

explicitly, the system perturbation $\Psi_1(\cdot)$ is obtained as

$$\begin{aligned}\Psi_1(\cdot) = &-\frac{D}{H}\left[-\frac{D}{H}(\omega-\omega_0)+\frac{\omega_0}{H}\left(P_{\rm m}-\frac{E'_{\rm q}V_{\rm s}\sin\delta}{X'_{\rm d\Sigma}+X_{\rm tcsc0}}\right)\right]-\frac{\omega_0 V_{\rm s}}{H(X'_{\rm d\Sigma}+X_{\rm tcsc0})}\\ &\times\left[E'_{\rm q}(\omega-\omega_0)\cos\delta+\frac{\sin\delta}{T_{\rm d0}}\left(\frac{(X_{\rm d}-X'_{\rm d})(V_{\rm s}\cos\delta-E'_{\rm q})}{(X'_{\rm d\Sigma}+X_{\rm tcsc0})}-E'_{\rm q}\right)\right]\\ &-\frac{\omega_0 V_{\rm s}\sin\delta}{H(X'_{\rm d\Sigma}+X_{\rm tcsc0})}\times\frac{K_{\rm c}}{T_{\rm d0}}u_{\rm fd}-b_{10}u_{\rm fd}\end{aligned} \tag{21}$$

Defining a fictitious state as $z_4 = \Psi_1(\cdot)$, and the extended state variable is denoted as $z_{\rm e} = [z_1, z_2, z_3, z_4]^{\rm T}$, the fourth-order state equation is

$$\dot{z}_{\rm e} = A_1 z_{\rm e} + B_1 u_{\rm fd} + B_2\dot{\Psi}_1(\cdot) \tag{22}$$

where

$$A_1 = \begin{bmatrix} 0 & 1 & 0 & 0\\ 0 & 0 & 1 & 0\\ 0 & 0 & 0 & 1\\ 0 & 0 & 0 & 0\end{bmatrix},\qquad B_1 = \begin{bmatrix}0\\0\\b_{10}\\0\end{bmatrix},\qquad B_2 = \begin{bmatrix}0\\0\\0\\1\end{bmatrix}$$

A fourth-order HGSPO (8) is given as

$$\begin{cases} \dot{\hat{z}}_1 = \hat{z}_2 + \frac{\alpha_1}{\epsilon}(z_1 - \hat{z}_1) \\ \dot{\hat{z}}_2 = \hat{z}_3 + \frac{\alpha_2}{\epsilon^2}(z_1 - \hat{z}_1) \\ \dot{\hat{z}}_3 = \hat{\Psi}_1(\cdot) + \frac{\alpha_3}{\epsilon^3}(z_1 - \hat{z}_1) + b_{10}u_{\mathrm{fd}} \\ \dot{\hat{\Psi}}_1(\cdot) = \frac{\alpha_4}{\epsilon^4}(z_1 - \hat{z}_1) \end{cases} \tag{23}$$

Extending the TCSC dynamics, it yields

$$\begin{cases} \dot{y} = \Psi_{\mathrm{tcsc}}(\cdot) + b_{20}u_{\mathrm{c}} \\ \dot{y}_2 = \dot{\Psi}_{\mathrm{tcsc}}(\cdot) \end{cases} \tag{24}$$

where

$$\Psi_{\mathrm{tcsc}}(\cdot) = -\frac{1}{T_{\mathrm{c}}}y + \frac{K_{\mathrm{T}}}{T_{\mathrm{c}}}u_{\mathrm{c}} - b_{20}u_{\mathrm{c}} + \zeta_{\mathrm{tcsc}} \tag{25}$$

A second-order HGPO (11) is used to obtain $\hat{\Psi}_{\mathrm{tcsc}}(\cdot)$ as

$$\begin{cases} \dot{\hat{y}} = \hat{\Psi}_{\mathrm{tcsc}}(\cdot) + \frac{\alpha_1'}{\epsilon}(y - \hat{y}) + b_{20}u_{\mathrm{c}} \\ \dot{\hat{\Psi}}_{\mathrm{tcsc}}(\cdot) = \frac{\alpha_2'}{\epsilon^2}(y - \hat{y}) \end{cases} \tag{26}$$

For system (1), one can obtain $\tilde{p}(z,y)$ from (21) according to (15) as

$$\tilde{p}(z,y) = \frac{\omega_0 V_\mathrm{s}}{H}\Big[\frac{1}{X_\Delta}\Big(\frac{-DE'_\mathrm{q}\sin\delta}{H} + E'_\mathrm{q}(\omega-\omega_0)\cos\delta + \frac{\sin\delta}{T_{\mathrm{d}0}} \times (-E'_\mathrm{q} + K_\mathrm{c}u_\mathrm{fd})\Big) + \frac{X'_\Delta}{X_\Delta^2}\frac{(X_\mathrm{d}-X'_\mathrm{d})(V_\mathrm{s}\cos\delta - E'_\mathrm{q})\sin\delta}{T_{\mathrm{d}0}}\Big] \tag{27}$$

where $X_\Delta = (X'_{\mathrm{d}\Sigma} + X_{\mathrm{tcsc}0} + y)(X'_{\mathrm{d}\Sigma} + X_{\mathrm{tcsc}0})$ and $X'_\Delta = (2X'_{\mathrm{d}\Sigma} + 2X_{\mathrm{tcsc}0} + y)$. The PECAPC-based EC and TCSC controller are

$$\begin{cases} u_\mathrm{fd} = \frac{1}{b_{10}}(-\hat{\Psi}_1(\cdot) - k_1\hat{z}_3 - k_2\hat{z}_2 - k_3\hat{z}_1) \\ u_\mathrm{c} = \frac{1}{b_{20}}(-\hat{\Psi}_\mathrm{tcsc}(\cdot) - c\hat{z}_3\tilde{p}(z,y) - k'y + \nu) \\ \nu = -\beta y \end{cases} \tag{28}$$

A known $\tilde{p}(z,y)$ is a fundamental assumption in coordinated passive control design [19], which contains the system states and parameters and needs to be cancelled for passivation. In real power system operations, the damping coefficient D is small compared to the system inertia H thus $|DE'_\mathrm{q}\sin\delta/H| \approx 0$, and $|\frac{X'_\Delta}{X_\Delta^2}(X_\mathrm{d}-X'_\mathrm{d})(V_\mathrm{s}\cos\delta - E'_\mathrm{q})| \ll |-E'_\mathrm{q} + K_\mathrm{c}u_\mathrm{fd}|$ during the transient process due to the large excitation control input u_fd, thus one can approximate $\tilde{p}(z,y)$ by ignoring the relatively small components. Denoting $\tilde{p}^*(z,y)$ as its

approximation, it gives

$$\tilde{p}^*(z,y) = \frac{\omega_0 V_\mathrm{s}}{H X_\Delta}\Big(E'_\mathrm{q}(\omega-\omega_0)\cos\delta + \frac{\sin\delta}{T_{\mathrm{d}0}}(-E'_\mathrm{q} + K_\mathrm{c}u_\mathrm{fd})\Big) \tag{29}$$

To this end, we replace $\tilde{p}(z,y)$ by its approximation $\tilde{p}^*(z,y)$, controller (28) becomes

$$\begin{cases} u_\mathrm{fd} = \frac{1}{b_{10}}(-\hat{\Psi}_1(\cdot) - k_1\hat{z}_3 - k_2\hat{z}_2 - k_3\hat{z}_1) \\ u_\mathrm{c}^* = \frac{1}{b_{20}}(-\hat{\Psi}_\mathrm{tcsc}(\cdot) - c\hat{z}_3\tilde{p}^*(z,y) - k'y + \nu) \\ \nu = -\beta y \end{cases} \tag{30}$$

Based on assumption *A1*, constants b_{10} and b_{20} must satisfy following inequalities when the generator operates within its normal region:

$$b_{10} < -\omega_0 V_\mathrm{s} K_\mathrm{c}\sin\delta/[2HT_{\mathrm{d}0}(X'_{\mathrm{d}\Sigma} + X_{\mathrm{tcsc}0})]$$

$$b_{20} > K_\mathrm{T}/(2T_\mathrm{c})$$

During the most severe disturbance, the electric power will reduce from its initial value to around zero within a short period of time, Δ. Thus the boundary values of the estimated system states can be obtained as $|\hat{z}_3| \leq \omega_0 P_\mathrm{m}/H$, $|\hat{\Psi}_1(\cdot)| \leq \omega_0 P_\mathrm{m}/(H\Delta)$, and $|\hat{\dot{\Psi}}_1(\cdot)| \leq \omega_0 P_\mathrm{m}/(H\Delta^2)$, respectively.

4.2. Controller Design for a Multimachine System

For multimachine system (2), we choose $y = X_{\mathrm{tcsc}} - X_{\mathrm{tcsc0}}$, $u_1 = u_{\mathrm{c}}$ and $u_{2i} = u_{\mathrm{fd}i}$. Setting $y = 0$ in the equivalent admittance matrix Y, the zero dynamics can be obtained. Choose $z_{i1} = \delta_i - \delta_{i0}$, $i = 1, 2, \ldots, n$, where δ_{i0} is the initial rotor angle of the ith generator. Differentiating z_{i1} until the excitation control input $u_{\mathrm{fd}i}$ appears explicitly, the system perturbation $\Psi_i(\cdot)$ is obtained as

$$\begin{aligned}\Psi_i(\cdot) = &-\frac{\omega_0}{2H_i}\Big[\frac{D_i}{\omega_0}\frac{d\omega_i}{dt} + E'_{\mathrm{q}i}\frac{dI_{\mathrm{q}i}}{dt} + \frac{I_{\mathrm{q}i} + 2G_{ii}E'_{\mathrm{q}i}}{T_{\mathrm{d0}i}}(-E'_{\mathrm{q}i} - (x_{\mathrm{d}i} - x'_{\mathrm{d}i})I_{\mathrm{d}i})\Big] \\ &- \frac{\omega_0(I_{\mathrm{q}i} + 2G_{ii}E'_{\mathrm{q}i})}{2H_iT_{\mathrm{d0}i}}u_{\mathrm{fd}i} - b_{10i}u_{\mathrm{fd}i} \end{aligned} \tag{31}$$

Defining a fictitious state as $z_{i4} = \Psi_i(\cdot)$, and the extended state variable is denoted as $z_{i\mathrm{e}} = [z_{i1}, z_{i2}, z_{i3}, z_{i4}]^{\mathrm{T}}$, the fourth-order state equation is

$$\dot{z}_{i\mathrm{e}} = A_{i1}z_{i\mathrm{e}} + B_{i1}u_{\mathrm{fd}i} + B_{i2}\dot{\Psi}_i(\cdot) \tag{32}$$

where

$$A_{i1} = \begin{bmatrix} 0 & 1 & 0 & 0 \\ 0 & 0 & 1 & 0 \\ 0 & 0 & 0 & 1 \\ 0 & 0 & 0 & 0 \end{bmatrix}, \qquad B_{i1} = \begin{bmatrix} 0 \\ 0 \\ b_{10i} \\ 0 \end{bmatrix}, \qquad B_{i2} = \begin{bmatrix} 0 \\ 0 \\ 0 \\ 1 \end{bmatrix}$$

A fourth-order HGSPO (8) is used for the ith generator as

$$\begin{cases} \dot{\hat{z}}_{i1} = \hat{z}_{i2} + \frac{\alpha_{i1}}{\epsilon}(z_{i1} - \hat{z}_{i1}) \\ \dot{\hat{z}}_{i2} = \hat{z}_{i3} + \frac{\alpha_{i2}}{\epsilon^2}(z_{i1} - \hat{z}_{i1}) \\ \dot{\hat{z}}_{i3} = \hat{\Psi}_i(\cdot) + \frac{\alpha_{i3}}{\epsilon^3}(z_{i1} - \hat{z}_{i1}) + b_{10i}u_{\mathrm{fd}i} \\ \dot{\hat{\Psi}}_i(\cdot) = \frac{\alpha_{i4}}{\epsilon^4}(z_{i1} - \hat{z}_{i1}) \end{cases} \tag{33}$$

Let us consider the equivalent two-machine subsystem involving the TCSC device and denote them as the jth and kth machine, namely, the TCSC device is installed between the jth and kth machine. Furthermore, each machine denoted by the ith machine is equipped with its own EC. The extended TCSC dynamics is the same as system (24), and the same HGPO (26) is used to obtain $\hat{\Psi}_{\mathrm{tcsc}}(\cdot)$.

The PECAPC-based EC and TCSC controller for system (2) is

$$\begin{cases} u_{\mathrm{fd}i} = \frac{1}{b_{10i}}(-\hat{\Psi}_i(\cdot) - k_{i1}\hat{z}_{i3} - k_{i2}\hat{z}_{i2} - k_{i3}\hat{z}_{i1}) \\ u_{\mathrm{c}} = \frac{1}{b_{20}}(-\hat{\Psi}_{\mathrm{tcsc}}(\cdot) - c_j\hat{z}_{j3}\tilde{p}_j(z,y) - c_k\hat{z}_{k3}\tilde{p}_k(z,y) + \nu) \\ \nu = -\beta y, \qquad\qquad i = 1, 2, \cdots, n \end{cases} \tag{34}$$

where $\tilde{p}_j(z,y)$ and $\tilde{p}_k(z,y)$ are calculated from (31) according to (15), in which TCSC device is installed between the jth and kth machine. Thus one chooses $i = j$ and $i = k$ in (31) to calculate $\tilde{p}_j(z,y)$ and $\tilde{p}_k(z,y)$, respectively, using the values given in Appendix A. Similarly, in real power system operations, $|D_j E'_{\mathrm{q}j} E'_{\mathrm{q}k} \sin\delta_{jk}/(2H_j)| \approx 0$ as damping coefficient $D_j \ll H_j$, $|\frac{2G_{jj}}{T_{\mathrm{d}0j}}(x_{\mathrm{d}j} - x'_{\mathrm{d}j})| \ll |\omega_{jk}|$ as the self conductance G_{jj} is much smaller than time constant $T_{\mathrm{d}0j}$. Moreover $|(x_{\mathrm{d}k} - x'_{\mathrm{d}k})(\sum_{i=1,i\neq k,j}^{n} E'_{\mathrm{q}i} Y_{ki} \cos\delta_{ki} + \frac{X^{*'}_{\Delta}}{X^{*}_{\Delta}} E'_{\mathrm{q}j} \cos\delta_{jk})| \ll |u_{\mathrm{fd}k} - E'_{\mathrm{q}k}|$ and $|(x_{\mathrm{d}j} - x'_{\mathrm{d}j})(\sum_{i=1,i\neq j,k}^{n} E'_{\mathrm{q}i} Y_{ji} \cos\delta_{ji} + \frac{X^{*'}_{\Delta}}{X^{*}_{\Delta}} E'_{\mathrm{q}k} \cos\delta_{kj})| \ll |u_{\mathrm{fd}j} - E'_{\mathrm{q}j}|$ during the transient process due to the large excitation control inputs $u_{\mathrm{fd}k}$ and $u_{\mathrm{fd}j}$, thus one can approximate $\tilde{p}_j(z,y)$ and $\tilde{p}_k(z,y)$ by ignoring the relatively small components. Denoting their approximation as $\tilde{p}^*_j(z,y)$ and

$\tilde{p}_j^*(z,y)$, respectively, gives

$$\tilde{p}_j^*(z,y) = \frac{\omega_0 X_\Delta^*}{2H_j}\Big(\frac{E'_{\mathrm{q}k}}{T_{\mathrm{d}0j}}(u_{\mathrm{fd}j} - E'_{\mathrm{q}j})\sin\delta_{jk} + \frac{E'_{\mathrm{q}j}}{T_{\mathrm{d}0k}}(u_{\mathrm{fd}k} - E'_{\mathrm{q}k})\sin\delta_{jk} + E'_{\mathrm{q}j}E'_{\mathrm{q}k}\omega_{jk}\cos\delta_{jk}\Big)$$

$$\tilde{p}_k^*(z,y) = \frac{\omega_0 X_\Delta^*}{2H_k}\Big(\frac{E'_{\mathrm{q}j}}{T_{\mathrm{d}0k}}(u_{\mathrm{fd}k} - E'_{\mathrm{q}k})\sin\delta_{kj} + \frac{E'_{\mathrm{q}k}}{T_{\mathrm{d}0j}}(u_{\mathrm{fd}j} - E'_{\mathrm{q}j})\sin\delta_{kj} + E'_{\mathrm{q}k}E'_{\mathrm{q}j}\omega_{kj}\cos\delta_{kj}\Big)$$

As a result, one can replace $\tilde{p}_j(z,y)$ and $\tilde{p}_k(z,y)$ by their approximation $\tilde{p}_j^*(z,y)$ and $\tilde{p}_k^*(z,y)$, respectively. Controller (34) becomes

$$\begin{cases} u_{\mathrm{fd}i} = \frac{1}{b_{10i}}(-\hat{\Psi}_i(\cdot) - k_{i1}\hat{z}_{i3} - k_{i2}\hat{z}_{i2} - k_{i3}\hat{z}_{i1}) \\ u_{\mathrm{c}}^* = \frac{1}{b_{20}}(-\hat{\Psi}_{\mathrm{tcsc}}(\cdot) - c_j\hat{z}_{j3}\tilde{p}_j^*(z,y) - c_k\hat{z}_{k3}\tilde{p}_k^*(z,y) + \nu) \\ \nu = -\beta y, \qquad\qquad i = 1,2,\cdots,n \end{cases} \tag{35}$$

Similar to the SMIB case, constants b_{10i} and b_{20} are chosen to be:

$$b_{10i} < -\omega_0(I_{\mathrm{q}i} + 2G_{ii}E'_{\mathrm{q}i})/(2H_iT_{\mathrm{d}0i})$$

$$b_{20} > K_{\mathrm{T}}/(2T_{\mathrm{c}})$$

Moreover, estimates of state and perturbation are bounded as $|\hat{z}_{i3}| \leq \omega_0 P_{\mathrm{m}i}/(2H_i)$, $|\hat{\Psi}_i(\cdot)| \leq \omega_0 P_{\mathrm{m}i}/(2H_i\Delta)$, and $|\hat{\dot{\Psi}}_i(\cdot)| \leq \omega_0 P_{\mathrm{m}i}/(2H_i\Delta^2)$.

To this end, a decentralized EC can be obtained for the ith machine as only the measurement of its rotor angle δ_i is required, which can effectively handle the modelling uncertainties. The TCSC controller measures the rotor angles δ_j and δ_k, excitation control inputs $u_{\mathrm{fd}j}$ and $u_{\mathrm{fd}k}$, transient voltages $E'_{\mathrm{q}j}$ and $E'_{\mathrm{q}j}$. The nominal values of time constant $T_{\mathrm{d0}j}$ and $T_{\mathrm{d0}k}$, inertial constants H_j and H_k of the jth and kth machine, and transmission line reactance X_{jk} are used for coordination. Note that the difference between the nominal values and the real values of the system parameters are aggregated into the perturbation, which is estimated by PO.

5. Simulation Results

5.1. Evaluation on a Single Machine Infinite Bus System

A proportional-integral-derivative (PID) based TCSC controller and automatic voltage regulator equipped with lead-lag (LL) based PSS (PID+LL), CAPC used in [24], and PECAPC are compared. The system parameters and initial operating conditions are given in Appendix A. Through trial-and-error, we put the system poles to the left half plane to ensure the system stability

and dynamical performance. PECAPC parameters are chosen as: $k_1 = 9$, $k_2 = 27$, $k_3 = 27$ so as to place the poles of the linear system at $\xi = -3$; $b_{10} = -15$, $b_{20} = 100$, $k' = 5$, $\beta = 15$, $c = 0.001$; $\alpha_1 = 160$, $\alpha_2 = 9.6 \times 10^3$, $\alpha_3 = 2.56 \times 10^5$ and $\alpha_4 = 2.56 \times 10^6$ so as to place all the poles of the HGSPO at $\lambda = -40$; $\alpha_1' = 30$ and $\alpha_2' = 225$ so as to place all the poles of the HGPO at $\lambda' = -15$, $\epsilon = 0.1$ and $\Delta = 0.05$ s. The system variables are used in the per unit (p.u.) system. In the power systems analysis field of electrical engineering, per unit system is the expression of system quantities as fractions of a defined base unit quantity, which means the values have been normalized [1]. In this paper, assume the independent base values are active power P_{base}=1.0 p.u. and voltage V_{base}=1.0 p.u..

A three-phase short circuit fault occurs at $t = 1.0$ s and cleared at $t = 1.1$ s, where $|u_{\text{fd}}| \leq 7$ p.u., and $|X_{\text{tcsc}}| \leq 0.1$ p.u. such that a maximum 20% compensation ratio is implemented. Figure A.4 shows system responses with the EC alone, coordinated EC and TCSC controller (28) and its approximated controller (30), respectively. From which the effectiveness of coordination is verified as an extra system damping is injected, and the excitation control cost is reduced. Moreover, the approximation is valid as it can capture the main feature of the exact coordination, hence the approximated controllers

will be used for the rest of the studies.

System responses under the nominal model is illustrated by Fig. A.5. It is found that PECAPC can effectively stabilize the system. Figure A.6 presents system responses under a nonlinear unmodled TCSC dynamics $\zeta_{\text{tcsc}} = 10\sin(X_{\text{tcsc}} - X_{\text{tcsc0}})$, which is the same unmodelled TCSC dynamics used in [24] for the purpose of their control performance evaluation. However, PECAPC does not require the model error to satisfy this linear growth condition required by CAPC [24]. In fact, a general unmodelled TCSC dynamics can be estimated online by PO. PID+LL control performance degrades dramatically as it is not robust to the TCSC modelling uncertainty. In contrast, both CAPC and PECAPC can maintain a consistent control performance as this uncertainty is considered during control design.

The low frequency inter-area oscillation has been well defined in the power system research, which is caused by the dynamic interactions, in a low frequency, between multiple groups of generators. It results in a degrade of power system stability and must be suppressed. A typical inter-area oscillation $V_{\text{s}} = 1 + 0.1\sin(5t)$ is chosen to an corresponding oscillation frequency of $(2.5/\pi)$ Hz. System responses are given in Fig. A.7, the control performance of both PID+LL and CAPC degrades due to the external disturbance. In

contrast, PECAPC can effectively attenuate the inter-area oscillation.

5.2. Evaluation on a Three-Machine System

The PID+LL, CPC, where the real value of the states and perturbation is used in the controllers, and PECAPC (35) are then evaluated on a three-machine nine-bus system as shown in Fig. A.8, where a TCSC device is equipped between bus #7 and bus #8. The system parameters, initial operating conditions and PID+LL parameters are all given in Appendix A. PECAPC parameters are $b_{10i} = -30$, $k_{i1} = 15$, $k_{i2} = 75$, $k_{i3} = 125$ so as to place the poles of the linear system at $\xi = -5$; $b_{20} = 20$, $k' = 10$, $\beta = 1$ and $c_2 = c_3 = 0.25$; $\alpha_{i1} = 200$, $\alpha_{i2} = 1.5 \times 10^4$, $\alpha_{i3} = 5 \times 10^5$ and $\alpha_{i4} = 6.25 \times 10^6$ so as to place all the poles of the HGSPO at $\lambda = -40$; $\alpha'_1 = 60$ and $\alpha'_2 = 900$ so as to place all the poles of the HGPO at $\lambda' = -30$, $\epsilon = 0.1$ and $\Delta = 0.05$ s.

A three-phase short circuit occurs on one transmission line between bus #4 and bus #5 marked as point $'\times'$ at $t = 0.5$ s, the faulty transmission line is switched off at $t = 0.6$ s, and switched on again at $t = 1.1$ s when the fault is cleared, where $|u_{\mathrm{fd}i}| \leq 7$ p.u., and $|X_{\mathrm{tcsc}}| \leq 0.2$ p.u. such that a maximum 20% compensation ratio is implemented. Each generator is equipped with an EC.

System responses under operation type I are given by Fig. A.9, which shows PECAPC can achieve as satisfactory control performance as that of CPC when an accurate system model is completely known, their tiny difference is caused by the estimation error. The observer performance during the fault is also monitored, the estimation errors of HGSPO_1 and HGPO are given in Fig. A.10 and Fig. A.11, respectively, which show the observers can provide accurate estimates of system states with a fast tracking rate. However, there exists relatively larger errors in the estimate of perturbation at the instant of $t = 0.5\ s$, $t = 0.6\ s$, and $t = 1.1\ s$, this is due to the discontinuity in the equivalent admittance Y_{12} caused by the disconnection and reconnection of the transmission line 4-5(2) at the instant when the fault occurs.

A 50% increase of the generator inertia H_i, time constant $T_{\mathrm{d0}i}$ and TCSC time constant T_{c} used in controller (35) has been tested to evaluate the effect of parameter uncertainties on the dynamic response of the proposed control scheme with and without the PO. Fig. A.12 shows that the control performance degrades dramatically in the presence of parameter uncertainties without the PO, in contrast the same control performance can be achieved with the PO shown by Fig. A.13. This is because the parameter uncer-

tainties of the generator inertia H_i and time constant $T_{\mathrm{d}0i}$ are included in perturbation $\Psi_i(\cdot)$ (31), which is estimated by HGSPO (33) and compensated by controller (35). While the parameter uncertainties of the TCSC time constant T_{c} are included in perturbation $\Psi_{\mathrm{tcsc}}(\cdot)$ (25), which is estimated by HGPO (26) and compensated by controller (35).

The robustness of PID+LL, CPC and PECAPC has been evaluated by reducing the inertia constant H_i, time constant $T_{\mathrm{d}0i}$ of all generators and TCSC time constant T_{c} by 30% from their nominal values. System responses are provided in Fig. A.14, in which a big difference in CPC has been identified, with and without accurate parameters. By contrast, PID+LL and PECAPC remain satisfactory control performance as their design does not require accurate system parameters.

In order to test the general effectiveness of PECAPC, Figure A.15 presents system responses obtained with operation Type II and the above parameter uncertainties. In this case a larger active power is transmitted, and the system suffers more severe oscillation when the fault occurs. One can find PID+LL control performance degrades dramatically as its control parameters are based on local system linearization. On the other hand, a severe oscillation in CPC can be seen due to the system parameter uncertainty. In

contrast, PECAPC can maintain consistent control performance and provide significant robustness.

6. Hardware-in-the-loop Test

A HIL test has been undertaken based on dSPACE systems to verify the implementation feasibility of PECAPC. The configuration and experiment platform of HIL test are shown in Fig. A.17 and Fig. A.18, respectively. The EC and the TCSC controller are implemented on one dSPACE platform (DS1104 board) with a sampling frequency $f_{\mathrm{c}} = 1$ kHz, and the SMIB system is simulated on another dSPACE platform (DS1006 board) with a sampling frequency $f_{\mathrm{s}} = 10$ kHz. The measurements of the rotor angle δ, rotor speed ω, inner generator voltage E'_{q}, infinite bus voltage V_{s} and TCSC reactance X_{tcsc} are obtained from the real-time simulation of SMIB system on the DS1006 board, which are sent to two controllers implemented on the DS1104 board for calculating the control outputs, i.e., excitation voltage u_{fd} and TCSC modulated input u_{c}, respectively.

The disturbance is set up as: A 0.1 s three-phase short circuit fault occurs at 1.9 s. The total experiment time is 60 s and only the result of the first 8 s is presented for a clear illustration of the transient responses. The

following three tests are carried out: Test 1: Same observer parameters used in the previous simulation, which poles $\lambda = 40$, $\lambda' = 15$ with $b_{10} = -15$ and $b_{20} = 100$; Test 2: Reduced observer poles $\lambda = 15$, $\lambda' = 15$ with $b_{10} = -150$ and $b_{20} = 200$; and Test 3: Further reduced observer poles $\lambda = 5$, $\lambda' = 5$ with $b_{10} = -150$ and $b_{20} = 200$.

It has been found from Test 1 that an unexpected high-frequency oscillation occurs in u_{fd} and X_{tcsc}, which does not appear in the simulation. This is due to the large observer poles result in high gains, which lead to highly sensitive observer dynamics to the measurement disturbances. Hence reduced observer poles are chosen in Test 2. Fig. A.19 shows that the rotor angle and speed can be effectively stabilized, but a consistent high-frequency oscillation still exists in both u_{fd} and X_{tcsc}. Through the trial-and-error it finds that an observer pole in the range of 3-10 can avoid the high-frequency oscillation but with almost similar transient responses, therefore the observer poles are further reduced in Test 3. The system transient responses obtained in simulation and HIL test are given by Fig. A.20, one can find that the high-frequency oscillation disappears and the rotor angle and speed are still effectively stabilized.

The difference of the obtained results between the simulation and HIL test

is possibly caused by the following two reasons: (a) There exists measurement disturbances in the HIL test which are not considered in the simulation, a filter could be used to remove the measurement disturbances and improve the control performance; and (b) The discretization of the HIL test and sampling holding may introduce an additional amount of error compared to continuous control used in the simulation.

7. Discussion

It is necessary to study the computational cost of PECAPC as the high performance systems often have high computational cost. As the PECAPC needs to calculate a fourth-order HGSPO (23) and a second-order HGPO (26) together with a nonlinear function (29), it has the highest computational cost. The computational cost of CAPC is higher than that of CPC, as CAPC requires to solving an additional second-order parameter estimator (A.1). For CPC and PID+LL, it's difficult to compare the computational cost as CPC has to calculate three complex functions (21), (25) and (29), while PID+LL has to calculate a first-order integral used in PID, and a second-order lead-lag plus a first-order washout loop used in LL. For the multi-machine systems, the computational cost of CPC, CAPC (nonlinear functions

(21), (25) and (29) become more complex) and PECAPC (nonlinear function (29) becomes more complex) will be higher than that of the SMIB system, while the computational cost of PID+LL does not change. As the PECAPC is a decentralized controller, it can be easily extended into multimachine systems as each generator will be equipped with an individual EC, and the TCSC controller is separately implemented in the TCSC device.

Finally, the majority of studies related to power system control and operation is so far based on the simulation. The paper is concerned with the investigation of a new control method, for which it is difficult to undertake a physical experiment for the multi-machine power system due to its significant scale and complexity.

8. Conclusion

In this paper, a novel PECAPC has been proposed for synchronous generators and TCSC devices to improve the power system stability. It is able to fully exploit the physical properties of power systems through reshaping the distributed energies, and handle system uncertainties, unmodelled dynamics and external disturbances via perturbation estimation. The simulation results show that PECAPC can improve system damping and provide con-

sistent control performances under various operating conditions compared with conventional PID+LL, as the system nonlinearity is globally removed. Moreover, PECAPC has a simple structure as it needs only one coordination coefficient for each generator without an explicit CLF, thus it can be applied in complex and interconnected multimachine systems. Finally, compared with the accurate system model based CPC, greater robustness can be provided by PECAPC.

Acknowledgements

This work is supported by the China Scholarship Council (CSC), and National Key Basic Research and Development Program (973 Program, NO. 2012CB215100), China.

Appendix A. Controller Structures and System Parameters

The $\tilde{p}_j(z,y)$ and $\tilde{p}_k(z,y)$ used in controller (34) are

$$\tilde{p}_j(z,y) = \frac{\omega_0}{2H_j}\Big[\Big(\frac{-D_j E'_{\mathrm{q}j} E'_{\mathrm{q}k}\sin\delta_{jk}}{2H_j} + E'_{\mathrm{q}j}E'_{\mathrm{q}k}\omega_{jk}\cos\delta_{jk} + \frac{E'_{\mathrm{q}k}}{T_{\mathrm{d}0j}} \times (u_{\mathrm{fd}j} - E'_{\mathrm{q}j})\sin\delta_{jk}$$
$$+ \frac{2E'_{\mathrm{q}k}}{T_{\mathrm{d}0j}} G_{jj} E'_{\mathrm{q}j}(x_{\mathrm{d}j} - x'_{\mathrm{d}j})\cos\delta_{jk} + E'_{\mathrm{q}j} \times \frac{\sin\delta_{jk}}{T_{\mathrm{d}0k}}\Big(u_{\mathrm{fd}k} - E'_{\mathrm{q}k} + (x_{\mathrm{d}k} - x'_{\mathrm{d}k})$$
$$\times \sum_{i=1, i\neq k,j}^{n} E'_{\mathrm{q}i} Y_{ki}\cos\delta_{ki}\Big) + \frac{E'_{\mathrm{q}k}\sin\delta_{jk}}{T_{\mathrm{d}0j}}(x_{\mathrm{d}j} - x'_{\mathrm{d}j}) \sum_{i=1, i\neq k,j}^{n} E'_{\mathrm{q}i} Y_{ji}\cos\delta_{ji}\Big) X^*_\Delta + X^{*'}_\Delta$$
$$\times \Big(\frac{E'^2_{\mathrm{q}j}\sin(2\delta_{jk})}{2T_{\mathrm{d}0k}}(x_{\mathrm{d}k} - x'_{\mathrm{d}k}) + \frac{E'^2_{\mathrm{q}k}\sin(2\delta_{jk})}{2T_{\mathrm{d}0j}}(x_{\mathrm{d}j} - x'_{\mathrm{d}j})\Big)\Big]$$

$$\tilde{p}_k(z,y) = \frac{\omega_0}{2H_k}\Big[\Big(\frac{-D_k E'_{\mathrm{q}k} E'_{\mathrm{q}j}\sin\delta_{kj}}{2H_k} + E'_{\mathrm{q}k}E'_{\mathrm{q}j}\omega_{kj}\cos\delta_{kj} + \frac{E'_{\mathrm{q}j}}{T_{\mathrm{d}0k}} \times (u_{\mathrm{fd}k} - E'_{\mathrm{q}k})\sin\delta_{kj}$$
$$+ \frac{2E'_{\mathrm{q}j}}{T_{\mathrm{d}0k}} G_{kk} E'_{\mathrm{q}k}(x_{\mathrm{d}k} - x'_{\mathrm{d}k})\cos\delta_{kj} + E'_{\mathrm{q}k} \times \frac{\sin\delta_{kj}}{T_{\mathrm{d}0j}}\Big(u_{\mathrm{fd}j} - E'_{\mathrm{q}j} + (x_{\mathrm{d}j} - x'_{\mathrm{d}j})$$
$$\times \sum_{i=1, i\neq j,k}^{n} E'_{\mathrm{q}i} Y_{ji}\cos\delta_{ji}\Big) + \frac{E'_{\mathrm{q}j}\sin\delta_{kj}}{T_{\mathrm{d}0k}}(x_{\mathrm{d}k} - x'_{\mathrm{d}k}) \sum_{i=1, i\neq j,k}^{n} E'_{\mathrm{q}i} Y_{ki}\cos\delta_{ki}\Big) X^*_\Delta + X^{*'}_\Delta$$
$$\times \Big(\frac{E'^2_{\mathrm{q}k}\sin(2\delta_{kj})}{2T_{\mathrm{d}0j}}(x_{\mathrm{d}j} - x'_{\mathrm{d}j}) + \frac{E'^2_{\mathrm{q}j}\sin(2\delta_{kj})}{2T_{\mathrm{d}0k}}(x_{\mathrm{d}k} - x'_{\mathrm{d}k})\Big)\Big]$$

where $X_{jk} = Y_{jk}^{-1}$, $X^*_\Delta = 1/[(X_{jk} + y + X_{\mathrm{tcsc}0})X_{jk}]$, and $X^{*'}_\Delta = (y + X_{\mathrm{tcsc}0} + 2X_{jk})/[(X_{jk} + y + X_{\mathrm{tcsc}0})X_{jk}]^2$. The CAPC based EC and TCSC controller

used in [24] is

$$
\begin{cases}
u_{\mathrm{fd}} = \frac{T_{\mathrm{d0}}}{K_{\mathrm{c}}}\Big\{ z_2 \frac{\omega_0 V_{\mathrm{s}} \sin\delta}{H(X'_{\mathrm{d}\Sigma}+X_{\mathrm{tcsc0}})} - \frac{(X_{\mathrm{d}}-X'_{\mathrm{d}})(V_{\mathrm{s}}\cos\delta - E'_{\mathrm{q}})}{T_{\mathrm{d0}}(X'_{\mathrm{d}\Sigma}+X_{\mathrm{tcsc0}})} \\
+\frac{E'_{\mathrm{q}}}{T_{\mathrm{d0}}} - c_3 z_3 - x_2(x_3^* + E'_{\mathrm{q0}})\cot\delta + \frac{H(X'_{\mathrm{d}\Sigma}+X_{\mathrm{tcsc0}})}{\omega_0 V_{\mathrm{s}}\sin\delta}\times \\
\Big[x_2(1+c_1c_2+\dot{\hat{\theta}}) + (c_1+c_2+\hat{\theta})(\frac{\omega_0}{H}P_{\mathrm{m}} + \hat{\theta}x_2 - \\
\frac{\omega_0 E'_{\mathrm{q}} V_{\mathrm{s}}\sin\delta}{H(X'_{\mathrm{d}\Sigma}+X_{\mathrm{tcsc0}})}) \Big] \Big\} \\
u_{\mathrm{c}} = \frac{T_{\mathrm{c}}}{K_{\mathrm{T}}}\Big(\frac{-\omega_0 E'_{\mathrm{q}} V_{\mathrm{s}}\sin\delta}{HX_\Delta} z_2 + \frac{(X_{\mathrm{d}}-X'_{\mathrm{d}})(V_{\mathrm{s}}\cos\delta - E'_{\mathrm{q}})}{T_{\mathrm{d0}}X_\Delta} z_3 \\
-\hat{\psi}y + \nu \Big) \\
\dot{\hat{\theta}} = \gamma\left(z_2 - z_3 \frac{H(X'_{\mathrm{d}\Sigma}+X_{\mathrm{tcsc0}})(\hat{\theta}+c_1+c_2)}{\omega_0 V_{\mathrm{s}}\sin\delta} \right) x_2 \\
\dot{\hat{\psi}} = \rho y^2 \\
\nu = -\beta y
\end{cases}
\tag{A.1}
$$

where $x_1 = \delta - \delta_0$, $x_2 = \omega - \omega_0$, $x_3 = E'_{\mathrm{q}} - E'_{\mathrm{q0}}$, $x_2^* = -c_1 x_1$, $z_2 = x_2 - x_2^*$, $z_3 = x_3 - x_3^*$, $x_3^* = [H(X'_{\mathrm{d}\Sigma}+X_{\mathrm{tcsc0}})/(\omega_0 V_{\mathrm{s}}\sin\delta)][x_1 + (\omega_0/H)P_{\mathrm{m}} + (\hat{\theta}+c_1)x_2 + c_2 z_2] - E'_{\mathrm{q0}}$.

[1] Grigsby L. L., (2012). *Power system stability and control*. CRC Press, Boca Raton, FL, USA, Third edition

[2] Revel G., Len A. E., Alonso D. M., and Moiola J. L., (2010). Bifurcation analysis on a multimachine power system model. *IEEE Trans. Circuits*

Syst. I, Reg. Papers., *57*(4), 937–949.

[3] Wang Y., Cheng D., Liu Y., and Li C., (2004). Adaptive H_{inf} excitation control of multimachine power systems via the Hamiltonian function method. *Int. J. Control*, *77*(4), 336–350.

[4] Shen T. L., Mei S. W., Lu Q., Hu W., and Tamura K, (2003). Adaptive nonlinear excitation control with L-2 disturbance attenuation for power systems. *Automatica*, *39*(1), 81–89.

[5] Jiang L., Wu Q. H., and Wen J. Y., (2004). Decentralized nonlinear adaptive control for multi-machine power systems via high-gain perturbation observerd. *IEEE Trans. Circuits Syst. I, Reg. Papers*, *51*(10), 2052–2059.

[6] Jiang Y. & Jiang Z. P., (2012). Robust adaptive dynamic programming for large-scale systems with an application to multimachine power system. *IEEE Trans. Circuits Syst. II, Bri. Express*, *59*(10), 693–697.

[7] Yao W., Jiang L., Fang J.K., Wen J.Y. and Cheng S.J., (2014). Decentralized nonlinear optimal predictive excitation control for multimachine power systems. *Int. J. Electr. Pow. Energy Syst.*, *55*, 620–627.

[8] Manjarekar N. S., Banavar R. N., and Ortega R., (2010). Application of interconnection and damping assignment to the stabilization of a synchronous generator with a controllable series capacitor. *Int. J. Elect. Power Energy Syst.*, *32*, 63–70.

[9] Sun L. Y., Tong S. C., and Liu Y., (2011). Adaptive backstepping sliding mode H_∞ control of static var compensator. *IEEE Trans. Control Syst. Technol.*, *19*(5), 1178–1185.

[10] Panda S. and Padhy N. P., (2008). Optimal location and controller design of STATCOM for power system stability improvement using PSO. *J. Franklin Inst.*, *345*(2), 166–181.

[11] Lei X., Li X., and Povh D., (2001). A nonlinear control for coordinating TCSC and generator excitation to enhance the transient stability of long transmission systems. *Electr Power Syst Res.*, *59*(2), 103–109.

[12] Leung J. S. K., Hill D. J., and Ni Y. X., (2006). Global power system control using generator excitation, PSS, FACTS devices and capacitor switching. *Int. J. Elect. Power Energy Syst.*, *27*(5-6), 448–464.

[13] Amin K., Mohammad J. M., and Moein P., (2013). Coordinated design of STATCOM and excitation system controllers for multi-machine power

systems using zero dynamics method. *Int. J. Elect. Power Energy Syst.*, *49*(5-6), 269–279.

[14] Wang Y., Hill D. J., Middleton R. H., and Gao L., (2002). Robust nonlinear coordinated excitation and TCSC control for power systems. *IEE Proc. Gen. Tran. Dist.*, *149*(3), 367–372.

[15] Liu Q. J., Sun Y. Z., Shen T. L., and Song Y. H., (2003). Adaptive nonlinear co-ordinated excitation and STATCOM controller based on Hamiltonian structure for multimachine-power-system stability enhancement. *IET Control Theory Appl.*, *150*(3), 285–294.

[16] Mei S. W., Chen J., Lu Q., Yokoyama A., and Goto M., (2004). Coordinated nonlinear robust control of TCSC and excitation for multimachine systems. *Int. J. Control Theory Appl.*, *2*(1), 35–42.

[17] Ortega R., Van der Schaft A., Maschke I., and Gerardo E., (2001). Putting energyback in control. *IEEE Control Syst. Mag.*, *21*(2), 18–33.

[18] Verrelli C. M. and Damm G., (2010). Robust transient stabilization problem for a synchronous generator in a power network. *Int. J. Control*, *83*(4), 816–828.

[19] Larsena M., Jankovi M., and Kokotovi P. V., (2003). Coordinated passivation designs. *Automatica*, *39*, 335–341.

[20] Chen H., Ji H. B., Wang B., and Xi H. S., (2006). Coordinated passivation techniques for the dual-excited and steam-valve control of synchronous generators. *IEE Proc. Control Theory Appl.*, *153*(1), 69–73.

[21] Isidori A., (1995). Nonlinear control systems. *Berlin: Springer, 3rd edition.*

[22] Ortega R., Schaf A., Castanos F., and Astolfi A., (2008). Control by interconnection and standard passivity-based control of port-Hamiltonian systems. *IEEE Trans. Automat. Control*, *53*(11), 2527–2542.

[23] Jing Y., Guan Z. H., and Hill D. J., (2009). Passivity-based control and synchronization of general complex dynamical networks. *Automatica*, *45*(9), 2107–2113.

[24] Sun L. Y., Zhao J., and Dimirovski G. M., (2009). Adaptive coordinated passivation control for generator excitation and thyristor controlled series compensation system. *Control Eng. Pract.*, *17*, 766–772.

[25] Fang S. and Wang J., (2012). Coordinated control of generator excitation

and TCSC based on Hamilton energy function. *Power System Protection Con.*, *40*(15), 24–28.

[26] Kwon S. J. and Chung W. K., (2004). Perturbation compensator based robust tracking control and state estimation of mechanical systems. Springer, New York.

[27] Han J. Q., (2009). From PID to active disturbance rejection control. *IEEE Trans. Ind. Electron.*, *56*(3), 900–906.

[28] Jiang L., Wu Q. H., and Wen J. Y., (2002). Nonlinear adaptive control via sliding-mode state and perturbation observer. *IEE Proc. Control Theory Appl.*, *149*(4), 269–277.

[29] Wu Q. H., Jiang L., and Wen J. Y., (2004). Decentralized adaptive control of interconnected non-linear systems using high gain observer. *Int. J. Control*, *77*(8), 703–712.

[30] Chen J., Jiang L., Yao W., and Wu Q. H., (2014). Perturbation estimation based nonlinear adaptive control of a full-rated converter wind turbine for fault ride-through capability enhancement. *IEEE Trans. Power Syst.*, *29*(6), 2733–2743.

List of Tables

Table A.1: SMIB system parameters (in p.u.)

$V_{\mathrm{t}} = 0.9669$	$H = 7$	$D = 0.5$	$P_{\mathrm{m}} = 0.9$
$X_{\mathrm{t}} = 0.127$	$X_{\mathrm{L1}} = 0.173$	$X_{\mathrm{L2}} = 0.3122$	$X_{\mathrm{d}} = 1.863$
$X'_{\mathrm{d}} = 0.257$	$T_{\mathrm{d0}} = 6.9$	$T_{\mathrm{c}} = 0.06$	$K_{\mathrm{T}} = 20$
$K_{\mathrm{c}} = 1$	$V_{\mathrm{s}} = 1.0$	$\delta_0 = 0.5892$	$\omega_0 = 100\pi$
$X_{\mathrm{tcsc0}} = 0$			

Table A.2: Three-machine system generator parameters (in p.u.)

Parameters	G_1	G_2	G_3
x_{d}	1.86	1.67	1.75
x'_{d}	0.335	0.306	0.342
T_{d0}	6.9	6.9	6.9
H	5.25	4.5	4
D	2.5	2.5	2.5

Table A.3: Three-machine system transmission line parameters (in p.u.)

Line No.	Impedance
5-7	0.405
4-5(1)	0.23
4-5(2)	0.23
4-6	0.205
6-9	0.185
7-8	0.325
8-9	0.255
$P_{\mathrm{L1}} = 3.45$	$P_{\mathrm{L2}} = 2.55$
$P_{\mathrm{L3}} = 1.5$	

Table A.4: Three-machine system operation Type I

Generator	P(p.u.)	Q(p.u.)	V(p.u.)$\angle\theta(deg.)$
G_1	0.5821	0.9124	$1.1295\angle 0.0$
G_2	0.3577	0.8036	$1.034\angle 8.9$
G_3	0.1486	0.3040	$1.1372\angle -7.9$

Table A.5: Three-machine system operation Type II

Generator	P(p.u.)	Q(p.u.)	V(p.u.)$\angle\theta(deg.)$
G_1	0.5356	0.7052	$1.1488\angle 0.0$
G_2	0.6132	0.8533	$1.1171\angle 17.8$
G_3	0.1103	0.2965	$1.1524\angle -11.9$

Table A.6: SMIB system PID+LL parameters (in p.u.)

$T_{\mathrm{R}} = 0.01$	$K_{\mathrm{pss}} = 40$	$T_{\mathrm{w}} = 10$	$T_1 = 0.3$
$T_2 = 0.1$	$T_3 = 0.3$	$T_4 = 0.1$	$K_{\mathrm{I}} = -1$
$K_{\mathrm{D}} = -0.1$	$K_{\mathrm{e}} = 25$	$K_{\mathrm{P}} = -1$	

Table A.7: Three-machine system PID+LL parameters (in p.u.)

$T_{\mathrm{R}} = 0.01$	$K_{\mathrm{pss}} = 30$	$T_{\mathrm{w}} = 10$	$T_1 = 0.2$
$T_2 = 0.1$	$T_3 = 0.3$	$T_4 = 0.1$	$K_{\mathrm{I}} = -5$
$K_{\mathrm{D}} = -0.5$	$K_{\mathrm{e}} = 100$	$K_{\mathrm{P}} = -10$	

List of Figures

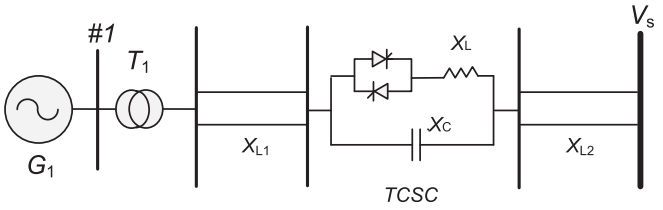

Figure A.1: The SMIB system equipped with a TCSC device.

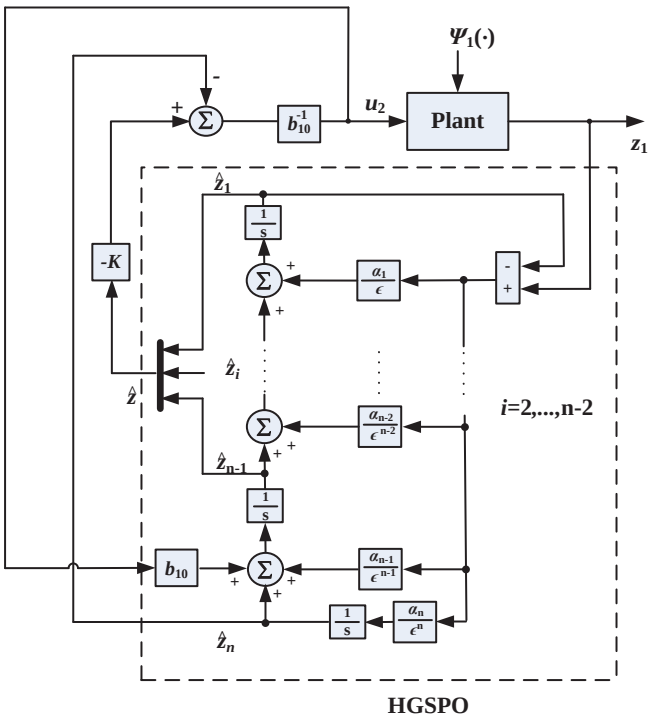

Figure A.2: The structure of stabilizing controller u_2.

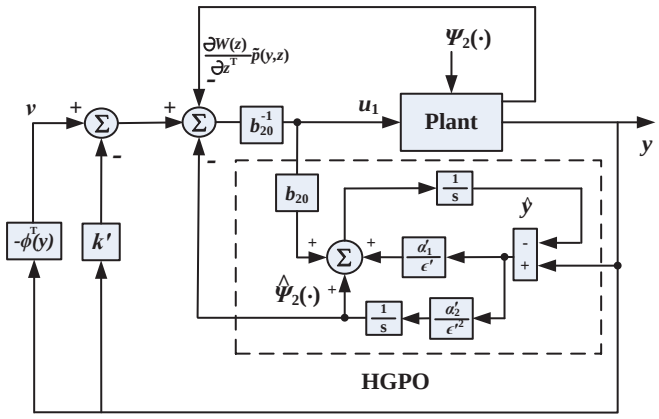

Figure A.3: The structure of coordinated controller u_1.

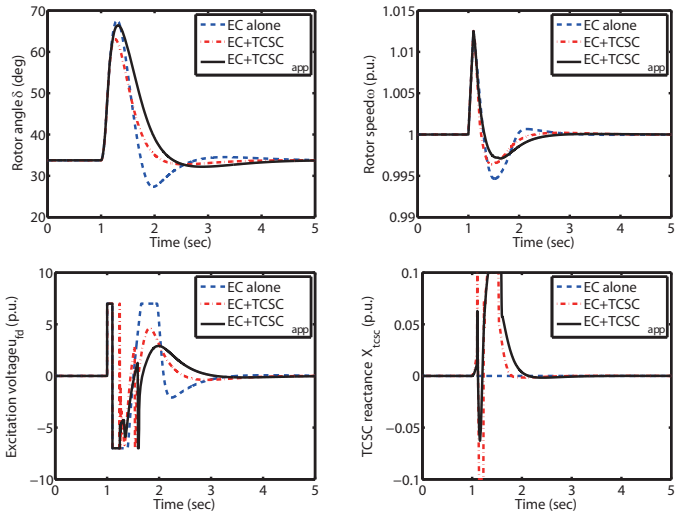

Figure A.4: System responses obtained with the EC alone, coordinated EC and TCSC controller, and approximated EC and TCSC controller in the SMIB system.

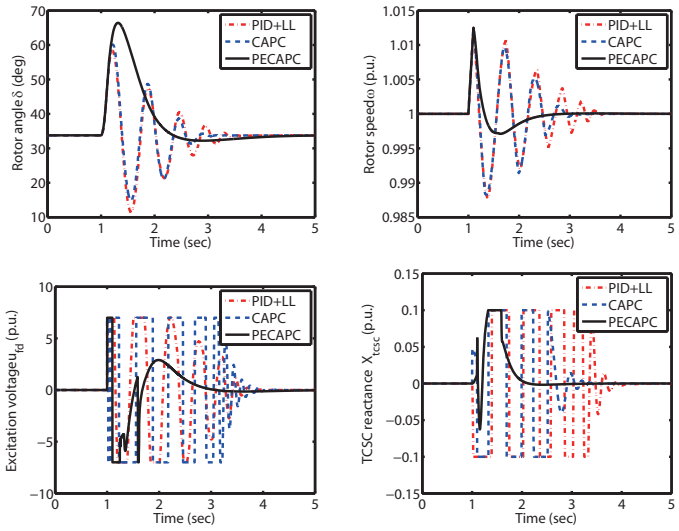

Figure A.5: System responses under the nominal model in the SMIB system.

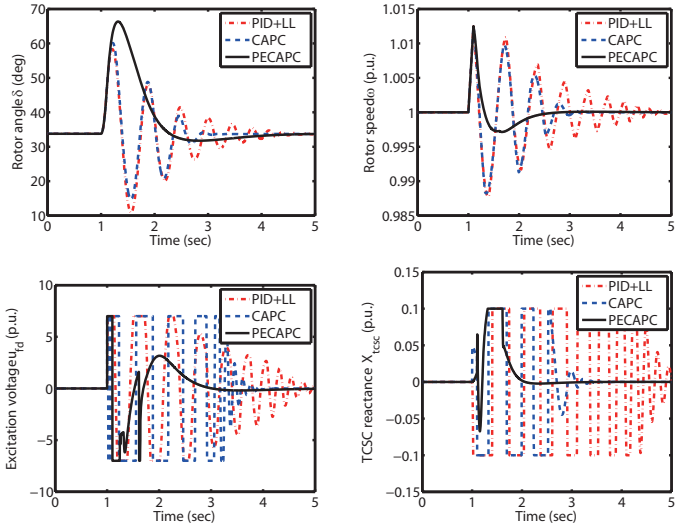

Figure A.6: System responses under an unmodelled TCSC dynamics $\zeta_{\text{tcsc}} = 10\sin(X_{\text{tcsc}} - X_{\text{tcsc0}})$ in the SMIB system.

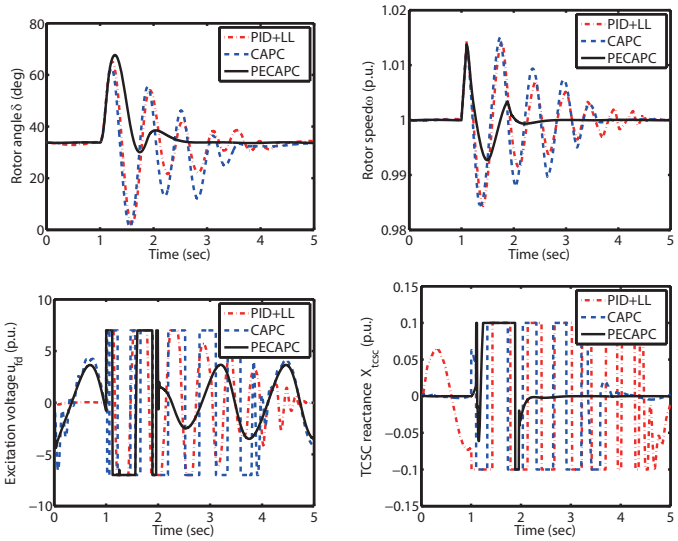

Figure A.7: System responses under an inter-area oscillation $V_{\mathrm{s}} = 1 + 0.1\sin(5t)$ in the SMIB system.

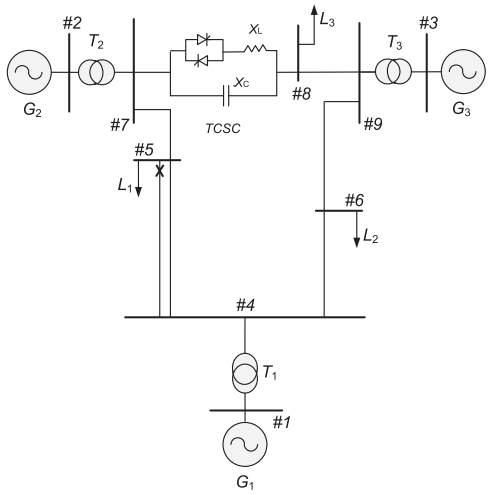

Figure A.8: The three-machine system equipped with a TCSC device.

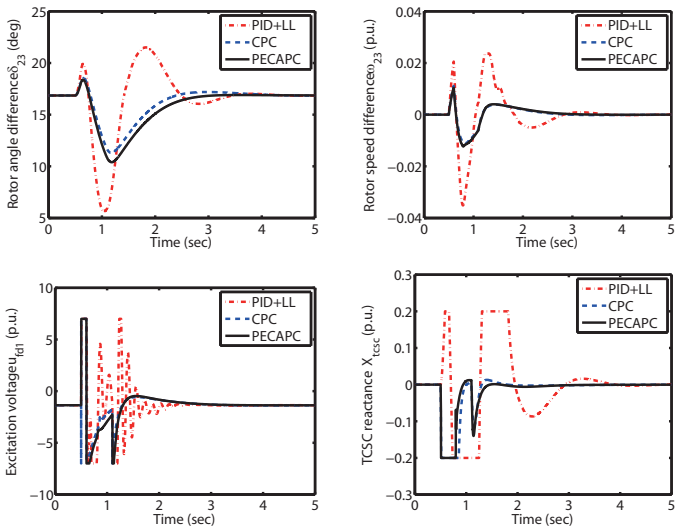

Figure A.9: System responses under operation Type I and the nominal model in the three-machine system.

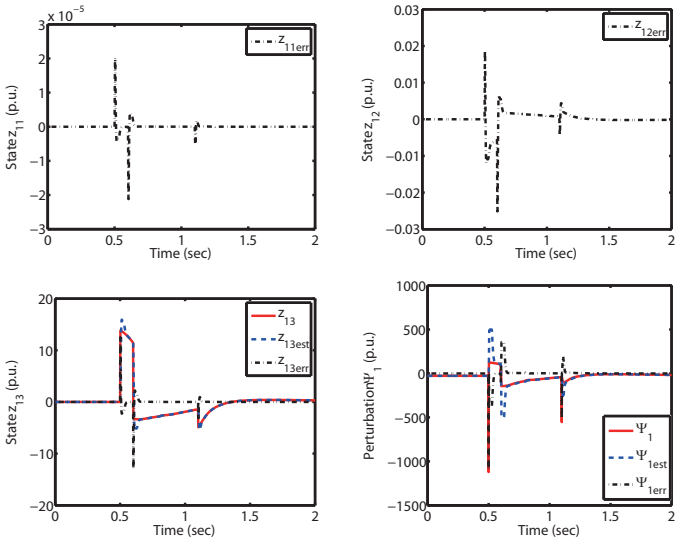

Figure A.10: Estimation errors of HGSPO_1 for G_1.

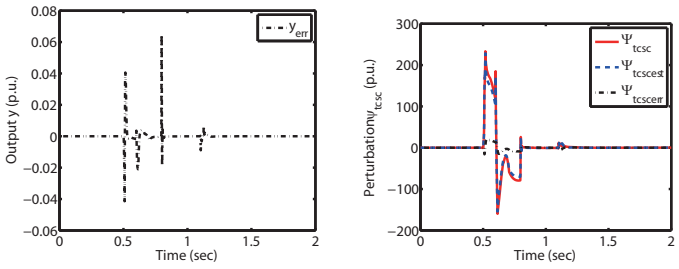

Figure A.11: Estimation errors of HGPO for TCSC.

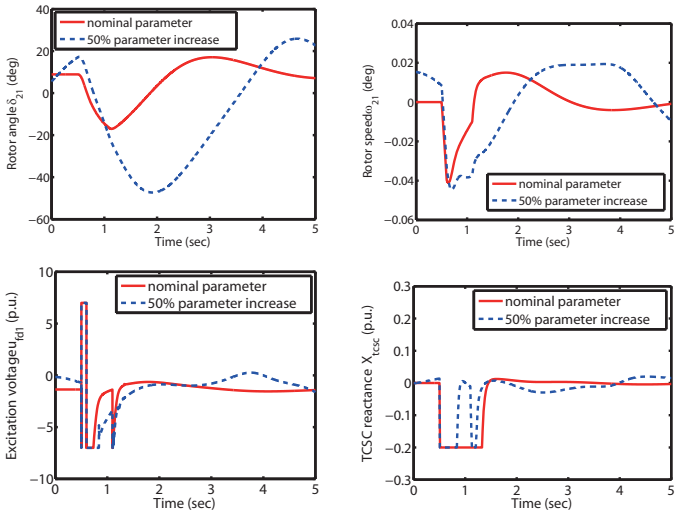

Figure A.12: The effect of a 50% parameter increases on the dynamic response of proposed controller without perturbation observer in the three-machine system.

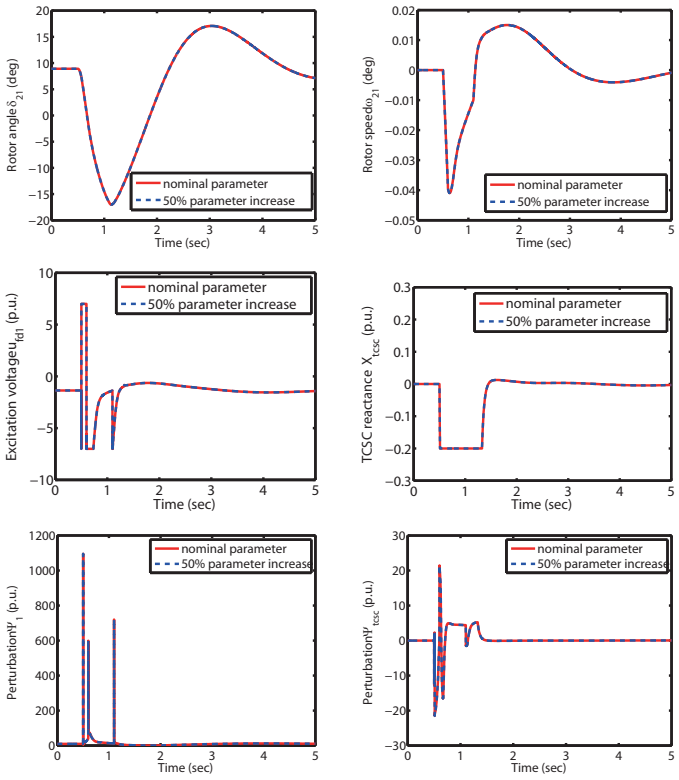

Figure A.13: The effect of a 50% parameter increases on the dynamic response of proposed controller with perturbation observer in the three-machine system.

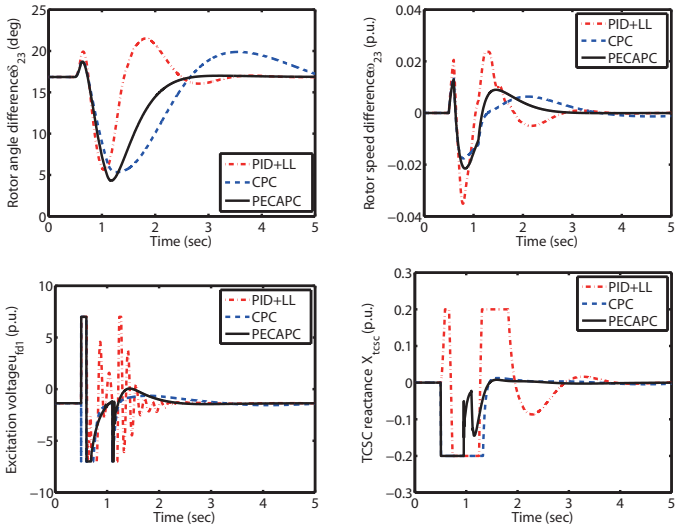

Figure A.14: System responses under operation Type I and the parameter uncertainties in the three-machine system.

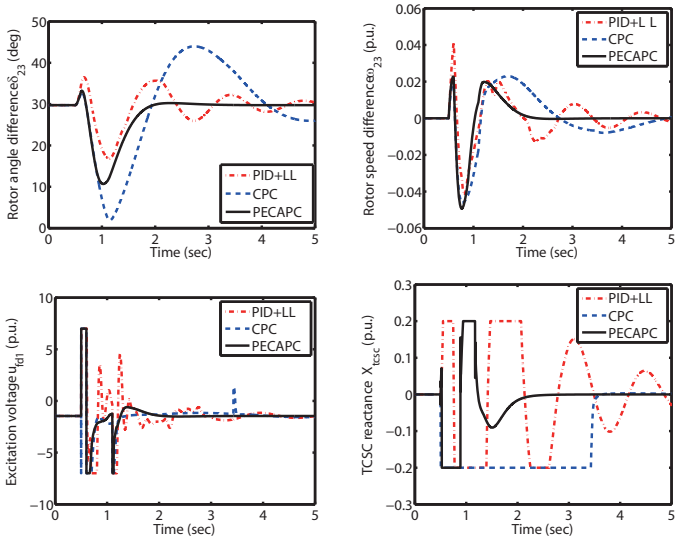

Figure A.15: System responses under operation Type II and the parameter uncertainties in the three-machine system.

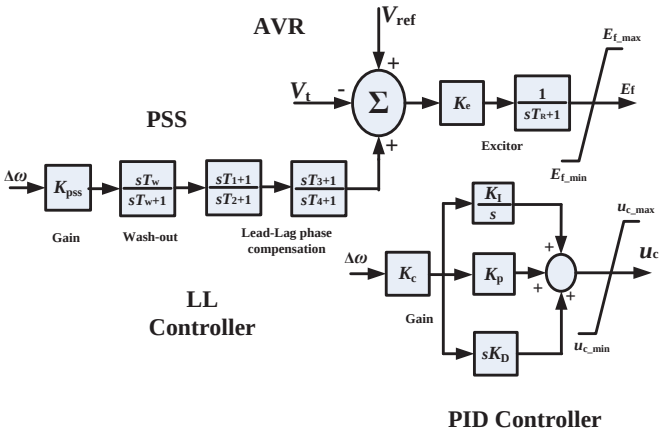

Figure A.16: The conventional PID+LL controller structure.

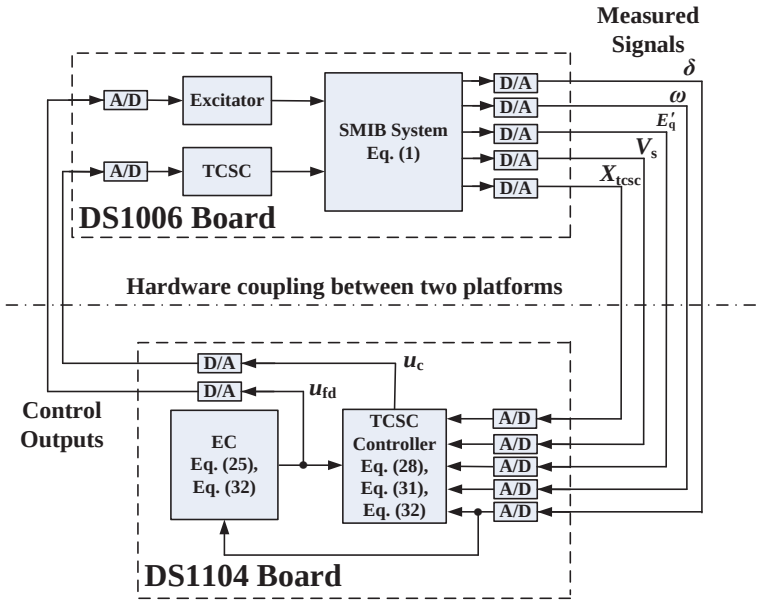

Figure A.17: The configuration of the hardware-in-the-loop test.

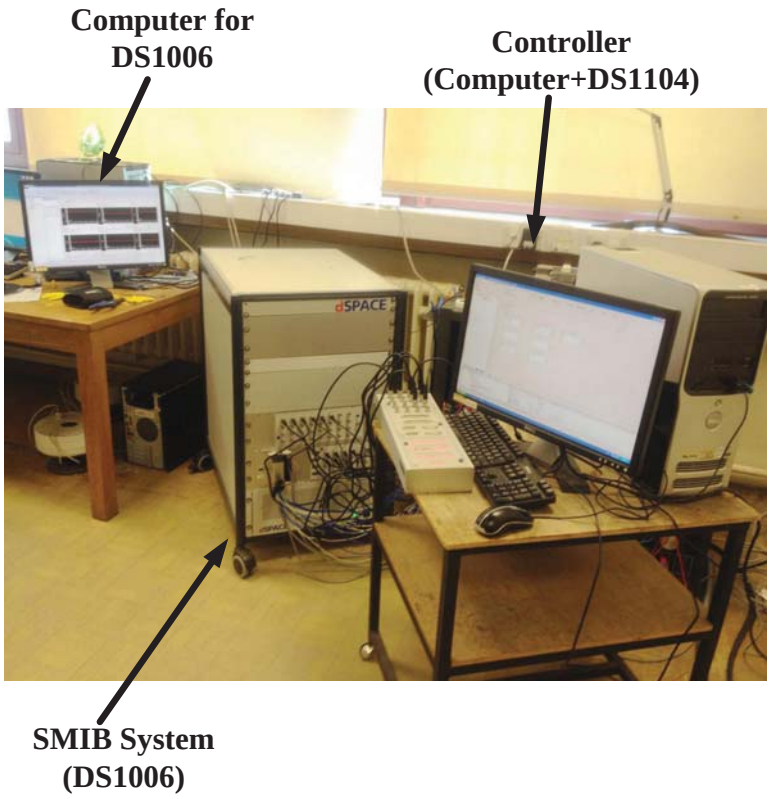

Figure A.18: The experiment platform of the hardware-in-the-loop test.

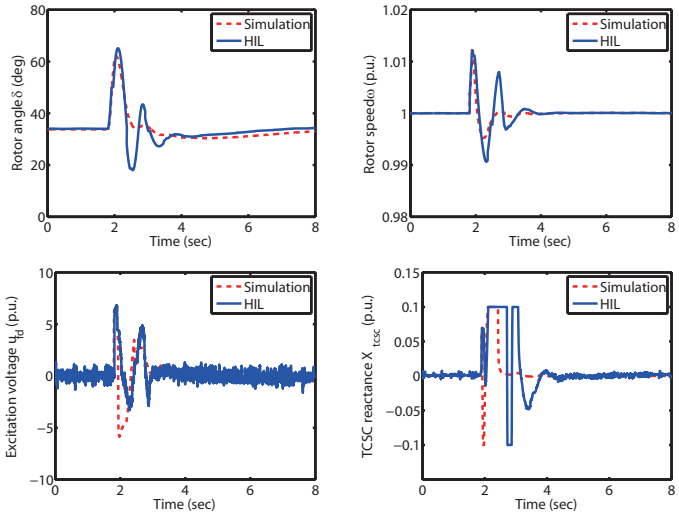

Figure A.19: PECAPC performances obtained in the hardware-in-the-loop test with large observer poles $\lambda = \lambda' = 15$.

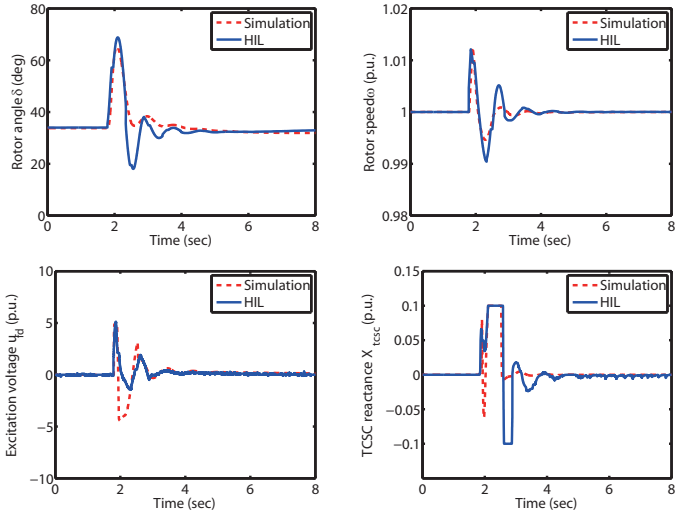

Figure A.20: PECAPC performances obtained in the hardware-in-the-loop test with proper observer poles $\lambda = \lambda' = 5$.